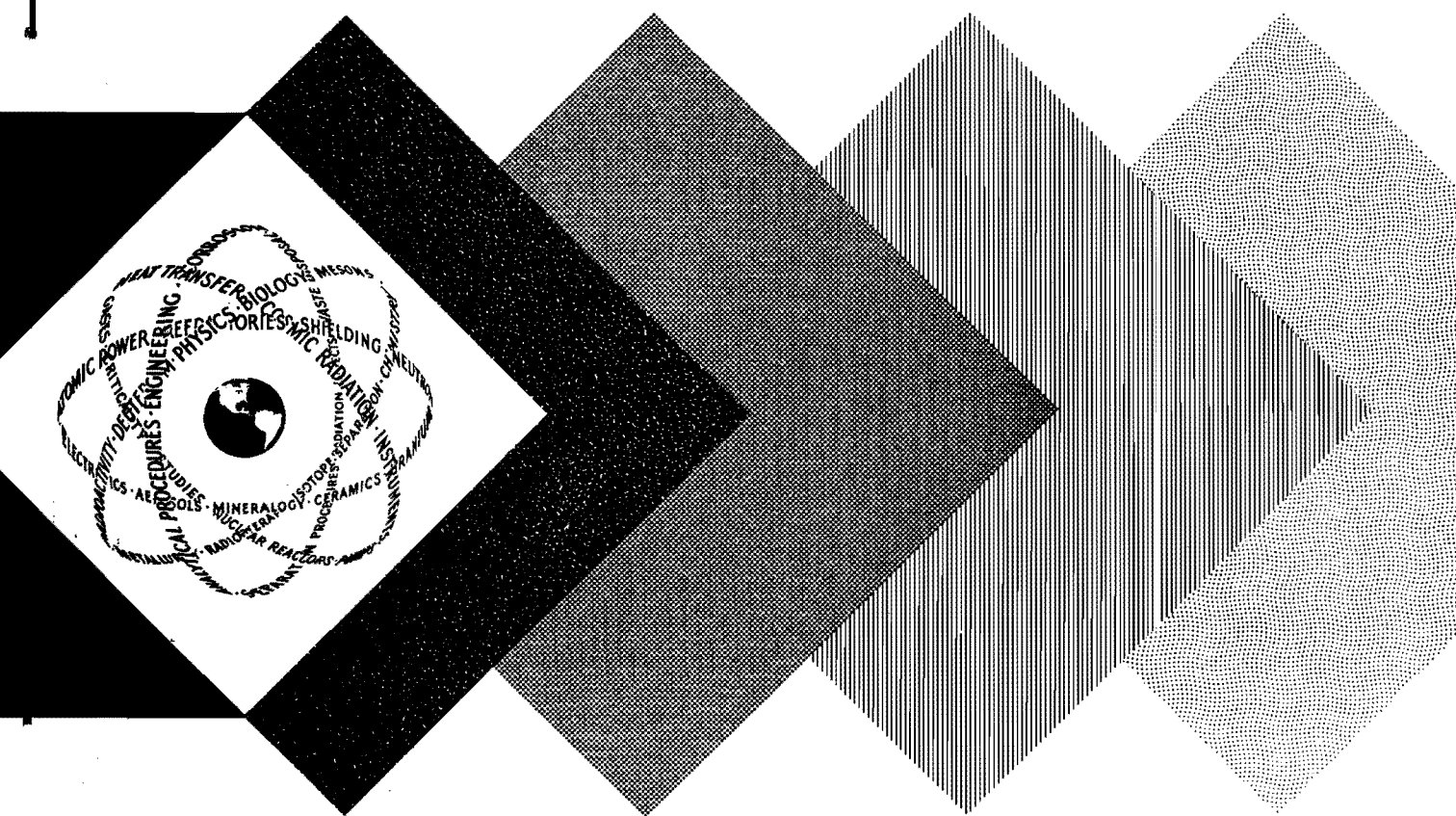# THE APPLICATION OF MICROWAVE TECHNIQUES TO STELLARATOR RESEARCH

By
Mark A. Heald

August 26, 1959

Project Matterhorn
Princeton University
Princeton, New Jersey

UNITED STATES ATOMIC ENERGY COMMISSION
Technical Information Service

LEGAL NOTICE

The Application of Microwave Techniques

to Stellarator Research

Mark A. Heald

August 26, 1959

Abstract

This report summarizes the basic principles of microwave diagnostics as applied to the highly-ionized, high-temperature plasmas encountered in controlled fusion devices, particularly stellarators. The first section discusses the electrical conductivity and the propagation of waves in an ionized gas. The second discusses methods of measurement of the high-frequency conductivity, with emphasis on the "free-space" optical technique appropriate for large, high-density plasmas. The third section deals with microwave radiation emitted by the plasma.

Table of Contents

I. INTRODUCTION

An ionized gas interacts strongly with electromagnetic fields at frequencies of the order of the plasma frequency[1]

$$\omega_p = \sqrt{\frac{ne^2}{\epsilon_o m}}$$

$$\frac{\omega_p}{2\pi} [kc] = 8.98 \sqrt{n[cm^{-3}]}$$

where n is the density of free electrons. For electron densities of interest in the controlled fusion field (excluding pinch and shock-wave devices), namely

$$10^{12} \lesssim n \lesssim 10^{15} \, cm^{-3},$$

the plasma frequency happens to lie in the microwave domain

$$9,000 \lesssim \frac{\omega_p}{2\pi} \lesssim 300,000 \, Mc$$

$$3 \, cm \gtrsim \lambda_p \gtrsim 1 \, mm.$$

Furthermore the electron cyclotron frequency

$$\omega_b = \frac{eB}{m}$$

$$\frac{\omega_b}{2\pi} \, [\,Mc\,] \;=\; 2.80 \; B \, [\,gauss\,],$$

for typical magnetic fields

$$5,000 \; \underset{\sim}{<} \; B \; \underset{\sim}{<} \; 50,000 \; gauss,$$

also lies in the microwave region

$$14,000 \; \underset{\sim}{<} \; \frac{\omega_b}{2\pi} \; \underset{\sim}{<} \; 140,000 \; Mc$$

$$2 \; cm \; \underset{\sim}{>} \; \lambda_b \; \underset{\sim}{>} \; 2 \, mm \, .$$

It therefore follows that microwave techniques are of great value in plasma research.

There are two broad classes of microwave experiments. First one can observe the propagation of microwaves in the plasma. The propagation characteristics depend principally upon electron density (n) and an effective collision rate (ν). From the time variation of density, together with collision frequency measurements, one can study the loss mechanisms in a decaying plasma (such as recombination, diffusion with or without a magnetic field, etc.). One can also study the position or motions of a plasma-vacuum boundary.

Secondly one can observe radiation emitted by the plasma. This second class is of importance because in general a plasma most closely approaches a blackbody at low frequencies and especially in the vicinity of the plasma and cyclotron frequencies, and also because the frequencies of certain types of collective motions of the plasma lie near the plasma frequency.

Historically the greatest interest in the interaction of electromagnetic radiation with ionized media has been in the field of radio propagation in the ionosphere.[2,3,4] Recently, the subject has become of importance to radio-astronomers.[5] Microwave techniques have also been used extensively in the field of classical gas discharges.[6] In the sense that one is dealing with a bounded, terrestial plasma sample, the detailed properties of which one desires to measure, this latter field is perhaps most akin to controlled fusion work. However, the relatively large size, high ionization, and high temperature of fusion plasmas often dictate different experimental approaches and introduce some features of ionospheric problems. The characteristics of hot and fully-ionized plasmas, in contrast to classical gas discharges, are (1) atomic excitation and ionization processes are negligible, (2) collisional damping effects are small or negligible, and (3) magnetohydrodynamic effects become significant.[7]

It should be noted that much the same types of physical information can be obtained by Langmuir probes[8] as by microwaves. The two techniques have quite different limitations however. The respective disadvantages can be listed as follows:

Disadvantages

Microwaves	Probes
difficulty of spatial resolution	physical perturbation of discharge
problems of boundary geometry and surroundings	difficulties due to sheath effects, plasma oscillations, and secondary emission
complications due to magnetic field	serious magnetic field complications
	physical damage of probe by hot plasma

II. ELECTRICAL PROPERTIES OF PLASMA

A. Resonance in a Free-Electron Gas

The physical nature of plasma oscillations can be seen from an argument originally given by Tonks and Langmuir.[1] For disturbances at sufficiently high frequencies the positive ions do not move and can be regarded as a continuous background charge. We consider an initially uniform electron gas of density n. By some external means a one-dimensional perturbation is introduced such that electrons at position x are displaced in the x-direction by a small increment ξ (x). The local density of electrons then departs from the uniform density n by the increment

$$\delta n = - n \frac{d\xi}{dx} .$$

Since the net charge density was originally zero, the perturbed charge density is

$$\delta\rho = -e\delta n = ne\frac{d\xi}{dx} .$$

Poisson's equation becomes

$$\epsilon_o \frac{dE}{dx} = ne\frac{d\xi}{dx} ,$$

which can be integrated immediately, giving

$$E = \frac{ne}{\epsilon_o} \xi$$

within an arbitrary constant. The force on the electron is then

$$F = -eE = -\frac{ne^2}{\epsilon_o} \xi ,$$

yielding the equation of motion

$$m\ddot{\xi} + \frac{ne^2}{\epsilon_o} \xi = F_{ext} ,$$

where F_{ext} is the external force required to produce the perturbation. If this

external force is suddenly removed, the electrons oscillate with simple harmonic

motion at the frequency

$$\omega_p{}^2 = \frac{ne^2}{\epsilon_o m} \ .$$

This oscillatory behavior is known as a plasma oscillation. The generalization

of this argument to three dimensions has been discussed by Dawson.[9]

The arbitrariness of the spatial distribution of ξ (x) in the above

argument implies that a plasma oscillation does not transfer energy; i.e., a

disturbance does not propagate beyond the region in which it is excited. This

property ceases to be true if a finite electron temperature exists,[10] or if the

plasma is bounded or contains gradients of electron density.[11, 12] In the case

of bounded plasmas, depolarizing effects displace macroscopic resonance from

the plasma frequency.[13,14]

The interaction of an electromagnetic wave with an electron gas can

be presented in the following simplified form. The equation of motion for an

electron under the influence of an electric field of frequency ω is

$$m \ \ddot{\xi} = - eE_o e^{-i \omega t}$$

the steady state solution of which is

$$\xi = \frac{e}{m\omega^2} \ \mathbf{E}_o e^{-i\omega t} \ .$$

The resulting current density is

$$J = -ne\ \xi = i\ \frac{ne^2}{m\omega}\ \mathbf{E}_o\ e^{-i\omega t} \ ,$$

corresponding to a conductivity

$$\sigma = i\ \frac{ne^2}{m\omega} \ .$$

The dispersion relation for plane waves varying as $\exp(\gamma x - i\omega t)$ in a medium of properties $(\epsilon_o, \mu_o, \sigma)$ is

$$-\gamma^2 = (\frac{\omega}{v_\phi})^2 = \frac{\omega^2}{c^2}\ (1+i\ \frac{\sigma}{\epsilon_o \omega}) \ ,$$

and thus the square of the index of refraction is

$$\mu^2 = (\frac{c}{v_\phi})^2 = 1 - \frac{ne^2}{\epsilon_o m \omega^2}$$

$$= 1 - \frac{\omega_p^2}{\omega^2} \ .$$

8

For low frequencies where

$$\omega^2 < \omega_p^2 \quad ,$$

the negative value of μ^2 signifies that a wave cannot propagate. If a wave impinges upon the plasma region from outside, it will be totally reflected at the boundary. For high frequencies where

$$\omega^2 > \omega_p^2 \quad ,$$

a wave propagates with phase velocity greater than c,

$$v_\phi = \frac{1}{(1 - \frac{\omega_p^2}{\omega^2})^{\frac{1}{2}}} \quad c.$$

The group velocity is of course less than c

$$v_g = \frac{\partial \omega}{\partial \beta} = \frac{c^2}{v_\phi} = (1 - \frac{\omega_p^2}{\omega^2})^{\frac{1}{2}} \quad c$$

which goes to zero when $\omega = \omega_p$.

When a damping force of the form $\quad - \nu m \dot{\xi}$

is included in the equation of motion, one obtains for the complex conductivity

$$\sigma = \frac{ne^2}{m} \frac{\nu + i\,\omega}{\omega^2 + \nu^2}$$

which is known as the Lorentz conductivity.

B. Conductivity of Plasma

It is customary to express the electromagnetic properties of a plasma in terms of a complex conductivity (see Appendix   ). As pointed out by Margenau,[15] the conductivity depends upon

(1) frequency ω

(2) electron density n

(3) collision rates $\nu\,(\omega)$

(4) electron velocity distribution $f\,(\omega)$

It also depends upon magnetic field, becoming a tensor quantity, but we temporarily postpone consideration of this factor. Using the Boltzmann equation, Margenau has obtained [15,16]

$$\sigma = -\frac{4\pi n e^2}{3 m} \int_o^\infty \frac{\nu + i\,\omega}{\omega^2 + \nu^2} \frac{d\,f\,(w)}{dw} w^3 \, d\,w. \qquad (1)$$

In the case of constant collision frequency (collision cross section inversely proportional to velocity), which is a good approximation in the case of

polarization forces between electrons and molecules, one obtains for any velocity

distribution the Lorentz conductivity formula

$$\sigma = \frac{ne^2}{m} \left[\frac{\nu + i\,\omega}{\omega^2 + \nu^2} \right] . \qquad (2)$$

In the case of a Maxwellian electron velocity distribution,

$$f(w) = \left(\frac{m}{2\pi k T} \right)^{3/2} e^{-\frac{mw^2}{2kT}} \qquad (3)$$

and arbitrary velocity-dependent collision frequency, one obtains

$$\sigma = \frac{8}{3\sqrt{\pi}} \frac{ne^2}{m} \int_0^\infty [\nu(u) + i\,\omega] \frac{u^4 e^{-u^2}\,du}{\omega^2 + \nu^2(u)} , \qquad (4)$$

where $u = \sqrt{\frac{m}{2kT}}\,w$. When $\nu^2 << \omega^2$, the Lorentz form can be recovered

by defining an effective collision rate [17]

$$\nu_{eff} \approx \frac{8}{3\sqrt{\pi}} \int_0^\infty \nu(u)\, u^4 e^{-u^2}\, du \qquad (\omega^2 >> \nu^2) . \qquad (5)$$

Similarly when $\omega^2 << \nu^2$,

$$\frac{1}{\nu_{eff}} \approx 3\frac{8}{\sqrt{\pi}} \int_{0}^{\infty} \frac{u^4 e^{-u^2} du}{\nu(u)} \qquad (\omega^2 << \nu^2). \quad (6)$$

The concept of effective collision frequency has been discussed by Ginsburg and by Molmud.[18]

As developed in the Appendix, we can write an equivalent complex dielectric constant

$$\kappa = 1 + i \frac{\sigma}{\omega e_o}$$

which becomes in the Lorentz case

$$\kappa = 1 - \frac{\omega_p^2}{\omega} \left[\frac{\nu - i\omega}{\omega^2 + \nu^2} \right]. \qquad (7)$$

The propagation constant for a plane wave in such a medium is

$$\gamma = \alpha + i\beta = i\sqrt{\kappa} \frac{\omega}{c} ,$$

from which we obtain

phase constant $\qquad \beta = \text{Re} \sqrt{\kappa} \frac{\omega}{c}$

$$\left. \right\} \quad (8)$$

attenuation constant $\qquad \alpha = -\operatorname{Im}\sqrt{\kappa}\ \dfrac{\omega}{c}$

$\left.\right\}$ (8)

absorption length
(skin depth) $\qquad \delta = -\dfrac{1}{\alpha} = \dfrac{1}{\operatorname{Im}\sqrt{\kappa}}\ \dfrac{c}{\omega}\ .$

Clearly in the absence of damping (i.e., $\nu \rightarrow 0$ and $T \rightarrow 0$) κ is real and γ is either pure real or pure imaginary.

C. Dissipative Processes in Ionized Gases

We have seen that the velocity dependence of the collision frequency for monentum transfer $\nu\ (\,w\,)$ and the electron velocity distribution function $f\ (\,w\,)$ must be known in order to relate the r.f. plasma conductivity and the microscopic physical quantities. The following table summarizes the common types of forces encountered and the resulting velocity dependence of the collision parameters:

interaction	force	velocity dependence		
		collision frequency $\nu = nsw$	cross section s	mean free path $\lambda = 1/ns$
electron-molecule.	hard sphere (step function)	w	1	1
	polarization $(1/r^5)$	1	$1/w$	w
electron-ion	Coulomb $(1/r^2)$	$1/w^3$	$1/w^4$	w^4

The cases of constant collision frequency and constant mean free path have been treated most fully in the literature since electro-molecule collisions are usually the dominant process in the classical (weakly ionized) gas discharge field.[19] The case of electron-ion collisions is much more subtle since the long-range nature of the Coulomb force requires careful consideration of the meaning of a collision rate (reciprocal relaxation time), as discussed by Spitzer.[20] However, this is clearly the damping process of greatest interest in highly ionized gases. In the presence of a magnetic field, electron-electron scattering influences the high-frequency conductivity, especially near the cyclotron resonance and at high densities.[21]

Let us first consider the effective collision frequency for high frequencies and Maxwellian distribution for

$$\nu (u) = \frac{K}{u^3} \, , \tag{9}$$

where K is a constant. We have from Eq. (5)

$$\nu_{eff} = \frac{8}{3\sqrt{\pi}} K \int_0^\infty u \, e^{-u^2} \, du$$

$$= \frac{4}{3\sqrt{\pi}} K \, . \tag{10}$$

Thus the effective collision frequency, to be used in the Lorentz formula at high frequencies, is that for an electron velocity

$$u = \left(\frac{3 \sqrt{\pi}}{4} \right)^{\frac{1}{3}}$$

or

$$w = \sqrt{\frac{2kT}{m}} \quad u = \sqrt{\left(\frac{9 \pi}{2}\right)^{\frac{1}{3}} \frac{kT}{m}}$$

which differs by less than three percent from the arithmetic mean speed

$$\bar{w} = \sqrt{\frac{8}{\pi} \frac{kT}{m}} .$$

The same procedure for low frequencies, from Equation (6), yields

$$\nu_{eff} = \frac{\sqrt{\pi}}{8} K , \qquad\qquad (11)$$

corresponding to the velocity

$$w = \sqrt{\frac{8}{\pi^{\frac{1}{3}}} \frac{kT}{m}} . ,$$

15

which is a factor of 1.5 greater than the mean speed (1.35 greater than

$$w_{rms} = \sqrt{3 \, \frac{kT}{m}} \,).$$

Spitzer defines a "90° deflection time" the reciprocal of which, for infinitely-massive positive ions, of charge Z, is [20]

$$\nu_D = \frac{8 \, \pi \, e^4}{(4\pi \epsilon_o)^2 m^2} \, \frac{n \, Z \, \ln \Lambda}{w^3} \, ,$$

(12)

where

$$\Lambda = \frac{3 \, (4\pi\epsilon_o)^{3/2}}{2 \sqrt{\pi} \, e^3} \, \frac{(kT)^{3/2}}{Z n^{\frac{1}{2}}}$$

is a cutoff applied to an integration over the impact parameter. For conditions of interest $\ln\Lambda$ is a slowly-varying quantity of the order of ten; we regard it as a constant in performing the integrations in Eqs. (5) and (6). Using Equation (12) to define K in Equation (9), we obtain

$$K = \frac{8\pi \, n \, e^4 \, \ln \Lambda}{(4\pi\epsilon_o)^2 m^2} \, (\frac{m}{2 \, k \, T})^{3/2}$$

(13)

and from Equations (10) and (11)

$$\nu_{eff} = \frac{8\sqrt{2\pi}}{3} \quad \frac{e^4}{(4\pi\epsilon_o)^2 m^{\frac{1}{2}}} \quad \frac{nZ\,\ln\Lambda}{(kT)^{3/2}} \qquad (\omega >> \nu) \qquad (14)$$

$$\nu_{eff} = \frac{\pi}{2\sqrt{2\pi}} \quad \frac{e^4}{(4\pi\epsilon_o)^2 m^{\frac{1}{2}}} \quad \frac{nZ\ln\Lambda}{(kT)^{3/2}} \qquad (\omega << \nu). \qquad (15)$$

The agreement of these two limits within a factor of 3.4 lends some credance to the utility of an effective collision frequency in the Lorentz formula.

An alternative approach to the effective collision frequency at low frequencies is to fit the Lorentz conductivity for $\omega << \nu$,

$$\sigma \rightarrow \frac{ne^2}{m} \frac{1}{\nu} \,,$$

to the Spitzer-Härm d.c. conductivity[20]

$$\sigma = \frac{4\sqrt{2\pi}\,(4\pi\epsilon_o)^2\,(kT)^{3/2}\,\gamma_e(Z)}{\pi^2\,m^{\frac{1}{2}}\,Ze^2\,\ln\Lambda} \,, \qquad (16)$$

where γ_e (Z) is a correction, of the order unity, due to electron-electron encounters. This procedure yields

$$\nu_{eff} = \frac{\pi^2}{4\sqrt{2\pi}} (4\pi\epsilon_o) \frac{e^4}{2m^{\frac{1}{2}}} \frac{n\,Z\,\ln\Lambda}{(kT)^{3/2}\gamma_E} \qquad (\omega=0) \qquad (17)$$

which differs by a factor of two from Equation (15).

An alternative approach at very high frequencies is to fit the attenuation constant derived from the Lorentz formula

$$- \alpha = Im \sqrt{1 + i\frac{\sigma}{\omega\epsilon_o}} \quad \frac{\omega}{c}$$

$$\longrightarrow \frac{1}{2} (\frac{\omega_p}{\omega})^2 \frac{\nu}{c} \qquad (\omega^2 >> \omega_p^2)$$

to the absorption coefficient for free-free transitions (inverse bremsstrahlung). This latter, modified for induced emission at low frequencies, $\hbar\omega << kT$, is [20, 22]

$$- \alpha = \frac{16\pi^2\sqrt{2\pi}}{3\sqrt{3}} \frac{e^6}{(4\pi\epsilon_o)^3 cm^3/2} \frac{n^2 Z\,\bar{g}}{\omega^2 (kT)^{3/2}} , \qquad (18)$$

where the averaged Gaunt factor $\bar{g}(\omega, n, Z, T)$,[23] a slowly varying parameter, is of the order of five for microwave frequencies.[24]

18

Equating the two attenuations, we have

$$\nu_{eff} = \frac{8\pi\sqrt{2\pi}}{3\sqrt{3}} \quad \frac{e^4}{(4\pi\epsilon_o)^2 m^{\frac{1}{2}}} \quad \frac{nZ\bar{g}}{(kT)^{3/2}} \quad . \qquad (\omega^2 >> \omega_p^2)$$

(19)

This is smaller than Equation (14) by the ratio

$$\frac{\pi \bar{g}}{\sqrt{3}\, \ln \Lambda} \quad \sim \quad 1.$$

Summarizing, we have for the effective collision frequency for electron-ion (Coulomb) collisions and a Maxwellian electron velocity distribution

$$\nu_{eff} = b \frac{e^4}{(4\pi\epsilon_o)^2 m^{\frac{1}{2}}} \quad \frac{nZ}{(kT)^{3/2}}$$

(20)

where the coefficient b has the following evaluations:

limit	model	b	approximate magnitude
$\omega = o$	Spitzer-Härm d.c. conductivity	$\dfrac{\pi^2 \ln \Lambda}{4\sqrt{2\pi}\,\gamma_E}$	.17
$\omega << \nu$	Spitzer 90° deflection time	$\dfrac{\pi^2 \ln \Lambda}{2\sqrt{2\pi}}$	.19
$\omega >> \nu$	Spitzer 90° deflection time	$\dfrac{8\sqrt{2\pi}\,\ln\Lambda}{3}$	.63
$\omega >> \omega_p$	free-free absorption	$\dfrac{8\pi\sqrt{2\pi g}}{3\sqrt{3}}$	.60

We conclude that a collision frequency of the form of Equation (20) can be used in the Lorentz formula (2) to give an approximation to the r.f. conductivity for all frequencies, except perhaps in the neighborhood of resonances such as the cyclotron and plasma frequencies.[21] Numerically, we have

$$\nu_{eff} \quad [\,\sec^{-1}\,] \sim 3\ 10^{-5}\ \frac{n[\,cm^{-3}\,]\ Z}{(kT\ [\,ev\,])^{3/2}}\ .$$

We note that the collision rate ("frequency") is to be compared with angular frequency. For typical values of

$$n \sim 6 \cdot 10^{13} \ cm^{-3}$$

$$kT \sim 10 \ ev$$

we have

$$\frac{\nu_{eff}}{2\pi} \sim 10 \ Mc$$

as compared with

$$\frac{\omega_p}{2\pi} \sim 70,000 \ Mc.$$

D. The Three Frequency Regions

We wish to consider as a function of frequency the electrical properties of a plasma characterized by the parameters ω_p ($\propto n^{\frac{1}{2}}$) and ν ($= \nu_{eff}$). We assume Lorentz conductivity (no magnetic field) and $\nu << \omega_p$. There are then three frequency regions.

(1) Low frequencies, $\omega < \nu$. The conductivity is

$$\sigma \approx \frac{ne^2}{m\nu}$$

independent of frequency. As in a metallic conductor, the resistive conduction current is large compared to the reactive displacement current as

$$\frac{\sigma_r}{\sigma_i + \omega \epsilon_o} = \frac{\nu/\omega}{1 + (\nu/\omega_p)^2} \approx \frac{\nu}{\omega} > 1.$$

The skindepth is

$$\delta = \frac{1}{\mathrm{Im}\sqrt{K}} \frac{c}{\omega} = \sqrt{\frac{2}{\mu_o \omega \sigma}} = \sqrt{\frac{2\nu}{\omega}} \frac{c}{\omega_p}. \qquad (21)$$

As in the usual skin-effect case the phase and attenuation constants are equal

$$\beta = -\alpha = \frac{1}{\delta} = \sqrt{\frac{\omega_p^2}{2\nu\omega}} \frac{\omega}{c} . \qquad (22)$$

We note that the conductivity increases with the three-halves power of the temperature. A one-kilovolt plasma is equivalent to room-temperature copper.

(2) Intermediate frequencies, $\nu < \omega < \omega_p$. The plasma will not propagate an electromagnetic wave, after the manner of a waveguide beyond cut-off. We have here

$$\delta = \frac{c}{\omega_p} \qquad (23)$$

$$\beta = \frac{\nu\omega_p}{2\omega^2} \quad \frac{\omega}{c} \, . \qquad (24)$$

(3) High frequencies, $\omega > \omega_p$. The plasma becomes a relatively lowloss dielectric:

$$\delta = \frac{2\omega^2}{\nu\omega_p} \quad \frac{c}{\omega_p} \qquad (25)$$

$$\beta = \left[1 - \left(\frac{\omega_p}{\omega} \right)^2 \right]^{\frac{1}{2}} \frac{\omega}{c} \, . \qquad (26)$$

with index of refraction

$$\mu = \frac{\beta c}{\omega} = \left[1 - \left(\frac{\omega_p}{\omega} \right)^2 \right]^{\frac{1}{2}} . \qquad (27)$$

The properties of these three regions change smoothly and slowly at the boundaries indicated with the exception of the skin depth across the plasma resonance, $\omega \approx \omega_p$. A fractional change in frequency of

$$\frac{\Delta \omega}{\omega} \sim (\frac{\nu}{\omega_p})^{\frac{1}{2}}$$

changes the plasma from opaque to transparent.

Figure 1 illustrates the dependence of electrical properties on frequency. The electron temperature of the plasma, shown as a parameter, determines the relative effective collision frequency.

For r.f. measurements in a time varying plasma the physical situation is better described with the following emphasis. Consider a fixed test frequency ω, to which there corresponds a critical density n_c defined by the plasma frequency relation

$$\omega^2 = \frac{n_c e^2}{\epsilon_o m} .$$ (28)

For densitites below this critical value the medium is a transparent dielectric; above, the medium is opaque and totally reflecting.

E. Magnetic Field Effects

When a plasma is located in a static magnetic field it becomes anisotropic on account of the gyroelectric behavior of the electrons. The conductivity is a tensor quantity. Propagation constants of waves depend upon the direction of propagation and the state of polarization.
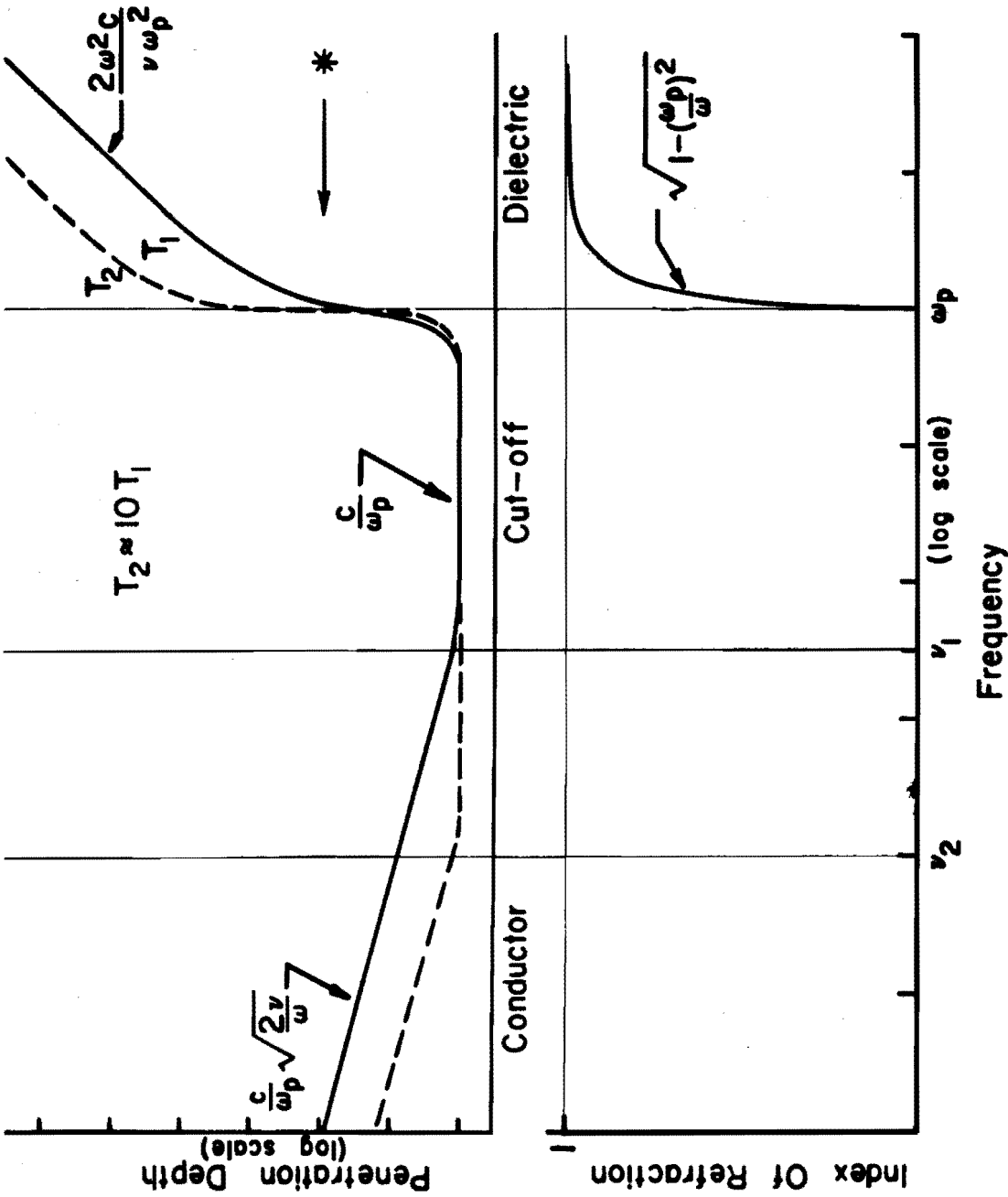
FIG. 1   Penetration depth and index of refraction of an electron gas as functions of frequency, neglecting positive ion, high temperature, and magnetic field effects. The effective electron-ion collision frequencies, ν_1 and ν_2, correspond to electron temperatures of about 10^4 and $10^5\,^\circ K$, respectively, in typical laboratory fully-ionized plasmas. The thickness of a typical plasma is indicated by the asterisk.

Considering explicitly the forces on an average electron, one obtains in analogy to the Lorentz formula the conductivity tensor [25]

$$||\sigma|| = \frac{ne^2}{2m} \begin{vmatrix} \ell + r & i(\ell-r) & 0 \\ -i(\ell-r) & \ell + r & 0 \\ 0 & 0 & 2p \end{vmatrix} \qquad (29)$$

where

$$p = \frac{1}{\nu - i\omega}$$

$$\left.\begin{array}{c} \ell \\ r \end{array}\right\} = \frac{1}{\nu - i(\omega \pm \omega_b)} \quad . \qquad (30)$$

The tensor is diagonal in rotating coordinates ($x \mp iy$, z):

$$||\sigma|| = \frac{ne^2}{m} \begin{vmatrix} \ell & 0 & 0 \\ 0 & r & 0 \\ 0 & 0 & p \end{vmatrix} . \qquad (31)$$

The dielectric constant becomes, in the usual fixed coordinates,

26

$$\|\kappa\| = \begin{vmatrix} \kappa_t & i\kappa_h & 0 \\ -i\kappa_h & \kappa_t & 0 \\ 0 & 0 & \kappa_p \end{vmatrix} \quad (32)$$

$$\kappa_p = 1 - \frac{\omega_p^2}{\omega} \frac{1}{\omega + i\nu} \qquad (E \parallel B_o) \quad \Big\}$$

$$\kappa_t = 1 - \frac{\omega_p^2}{\omega} \frac{\omega + i\nu}{(\omega + i\nu)^2 - \omega_b^2} \qquad (E \perp B_o) \quad \Big\} \quad (33)$$

$$\kappa_h = \frac{\omega_b^2}{\omega} \cdot \frac{\omega_b}{(\omega + i\nu)^2 - \omega_b^2} \qquad (\text{Hall}).$$

In the rotating coordinate, diagonalized system we have

$$\|\kappa\| = \begin{vmatrix} \kappa_\ell & 0 & 0 \\ 0 & \kappa_r & 0 \\ 0 & 0 & \kappa_p \end{vmatrix} \quad (34)$$

where

$$\kappa_\ell = 1 - \frac{\omega_p^\omega}{\omega} \frac{1}{(\omega + i\nu) + \omega_b} \qquad (35)$$

$$\kappa_r = 1 - \frac{\omega_p^2}{\omega} \frac{1}{(\omega + i\nu) - \omega_b}.$$

We note that

$$\kappa_t = \frac{\kappa_\ell + \kappa_r}{2}$$

$$\kappa_h = \frac{\kappa_\ell - \kappa_r}{2} .$$

When the dielectric constant tensor is substituted in the wave equation one obtains the following transcendental equation for the index of refraction μ : [*]

$$\tan^2 \theta = - \frac{\kappa_p \, (\mu^2 - \kappa_\ell)\,(\mu^2 - \kappa_r)}{(\mu^2 - \kappa_p)\,(\kappa_t \mu^2 - \kappa_\ell \kappa_r)} \qquad (36)$$

where θ is the angle between the direction of propagation and the magnetic field. Equation (36) is one form of the Appleton-Hartree formula, originally derived in connection with ionospheric propagation. [3,4] This form is particularly convenient because it allows us immediately to write down the indices of refraction in the special cases of propagation along and across the magnetic field:

---

[*] Strictly speaking μ^2 in this equation should be replaced by $- (\frac{\gamma c}{\omega})^2$, in the notation of the Appendix, and μ obtained from

$$\mu = \text{Im} \, (\frac{\gamma c}{\omega}) .$$

Since our chief interest here is in lossless media ($\nu \to 0$), we choose the simplified form.

Propagation along the field $(\theta = 0)$

$$-\left(\frac{\gamma c}{\omega}\right)^2 = \left\{\begin{array}{c} \kappa_\ell \\ \kappa_r \end{array}\right\} = 1 - \frac{\omega_p^2}{\omega} \frac{(\omega \pm \omega_b) - i\nu}{(\omega \pm \omega_b)^2 + \nu^2}$$

$$\xrightarrow[\nu=0]{} \frac{1 - \left(\frac{\omega_p}{\omega}\right)^2 \pm \frac{\omega_b}{\omega}}{1 \pm \frac{\omega_b}{\omega}} \ .$$

(37)

The two propagation constants correspond to two circularly polarized waves. A linearly polarized wave suffers a Faraday rotation of[26]

$$\tfrac{1}{2}\left(\beta_\ell - \beta_r\right).$$

(38)

Propagation across the field $(\theta = \pi/2)$

$$-\left(\frac{\gamma c}{\omega}\right)^2 = \kappa_p = 1 - \frac{\omega_p^2}{\omega} \frac{\omega - i\nu}{\omega^2 + \nu^2} \xrightarrow[\nu=0]{} 1 - \left(\frac{\omega_p}{\omega}\right)^2$$

(39)

and

$$- \left(\frac{\gamma c}{\omega}\right)^2 = \frac{\kappa_\ell \kappa_r}{\kappa_t} = 1 - \frac{\omega_p^2}{\omega(\omega + i\nu) - \dfrac{\omega^2 \omega_b^2}{\omega(\omega + i\nu) - \omega_p^2}}$$

$$= 1 - \frac{\omega_p^2 [(\omega^2 - \omega_p^2)(\omega^2 - \omega_p^2 - \omega_b^2) + \nu^2 \omega^2]}{\omega^2(\omega^2 - \omega_p^2 - \omega_b^2 - \nu^2)^2 + \nu^2(2\omega^2 - \omega_p^2)^2} \tag{40}$$

$$+ i \frac{\omega_p^2 \nu [\omega_p^4 + \omega^2(\omega^2 - 2\omega_p^2 + \omega_b^2 + \nu^2)]}{\omega[\omega^2(\omega^2 - \omega_p^2 - \omega_b^2 - \nu^2)^2 + \nu^2(2\omega^2 - \omega_p^2)^2]}$$

$$\xrightarrow{\vec{\nu}=0} \frac{[1 - (\frac{\omega_p}{\omega})^2]^2 - (\frac{\omega_b}{\omega})^2}{1 - (\frac{\omega_p}{\omega})^2 - (\frac{\omega_b}{\omega})^2} .$$

The first of these propagation constants corresponds to a linearly polarized wave polarized $E_{rf} \parallel B_o$, and is independent of magnetic field. The second, polarized $E_{rf} \perp B_o$, produces a separation of charge in the direction of propagation so that the wave is no longer TEM. The elliptical polarization produced by a superposition of these two waves is analogous to the Cotton-Mouton effect.

In the absence of collisions the propagation characteristics defined by the Appleton-Hartree formula can be expressed in terms of the following special frequencies:

$$\left. \begin{aligned} \omega_{\substack{1\\2}} &= \mp \frac{\omega_b}{2} + \sqrt{(\frac{\omega_b}{2})^2 + \omega_p^2} \\[2em] \omega_{bp} &= \omega_b^2 + \omega_p^2 \quad . \end{aligned} \right\} \quad (41)$$

In terms of these the principal propagation formulas become

$$\theta = 0:$$
$$\mu_{\substack{\ell\\r}}^2 = \frac{(\omega \mp \omega_1)(\omega \pm \omega_2)}{\omega(\omega \pm \omega_b)} \tag{42}$$

$$\theta = \frac{\pi}{2}:$$
$$\mu_\parallel^2 = 1 - (\frac{\omega_p}{\omega})^2 \tag{43}$$

$$\mu_\perp^2 = \frac{(\omega^2 - \omega_1^2)(\omega^2 - \omega_2^2)}{\omega^2(\omega^2 - \omega_{bp}^2)} \quad . \tag{44}$$

This formulation permits quick identification of the frequencies for cut-off $(\mu \to 0)$ and resonance $(\mu \to \infty)$.

A useful point of view in plasma physics is to regard electron density n, rather than frequency, as the independent variable. Introducing the notation

$$\eta \ = \ \frac{n}{n_c} \ = \ \left(\frac{\omega_p}{\omega}\right)^2$$

$$(45)$$

$$b \ = \ \frac{\omega_b}{\omega}$$

where the critical density is a measure of frequency defined by

$$n_c \ = \ \frac{\epsilon_o \, m \, \omega^2}{e^2} \quad , \qquad (46)$$

the relations (41) become

$$\eta_{\frac{1}{2}} \ = \ 1 \overset{+}{\underset{-}{}} b$$

$$\left.\begin{array}{c} \\ \\ \end{array}\right\} \qquad (47)$$

$$\eta_{bp} \ = \ 1 - b^2 \, .$$

We can now write the principal propagation constants in the following forms

$\theta = 0:$

$$\mu_{\ell_r}^2 \ = \ \frac{1 - \eta \overset{+}{\underset{-}{}} b}{1 \overset{+}{\underset{-}{}} b}$$

$$= \ 1 - \frac{\eta}{1 \overset{+}{\underset{-}{}} b} \qquad (48)$$

$$= \ \frac{(\eta_1 - \eta)}{\eta_{\frac{1}{2}}}$$

$$\theta = \frac{\pi}{2}:$$

$$\mu_{\parallel}^2 = 1 - \eta \tag{49}$$

$$\mu_{\perp}^2 = \frac{(1 - \eta)^2 - b^2}{1 - \eta - b^2} \tag{50}$$

$$= \frac{(\eta_1 - \eta)(\eta_2 - \eta)}{(\eta_{bp} - \eta)} \quad .$$

We note that for strong magnetic fields where

$$b = \frac{\omega_b}{\omega} > 1$$

η_2 and η_{bp} become negative, so that the respective cut-offs and resonances at $\eta = \eta_2$ and η_{bp} no longer occur in (48) and (50).

Figure 2 illustrates qualitatively the behavior of these propagation constants as a function of density. The features to be noted are the magnetic field dependence of the cutoff densities (where $\mu \to 0$), and the existence of the upper "passband" in the $\mu_{\perp}^2$ case for

$$1 - b^2 < \eta < 1 + b \quad .$$
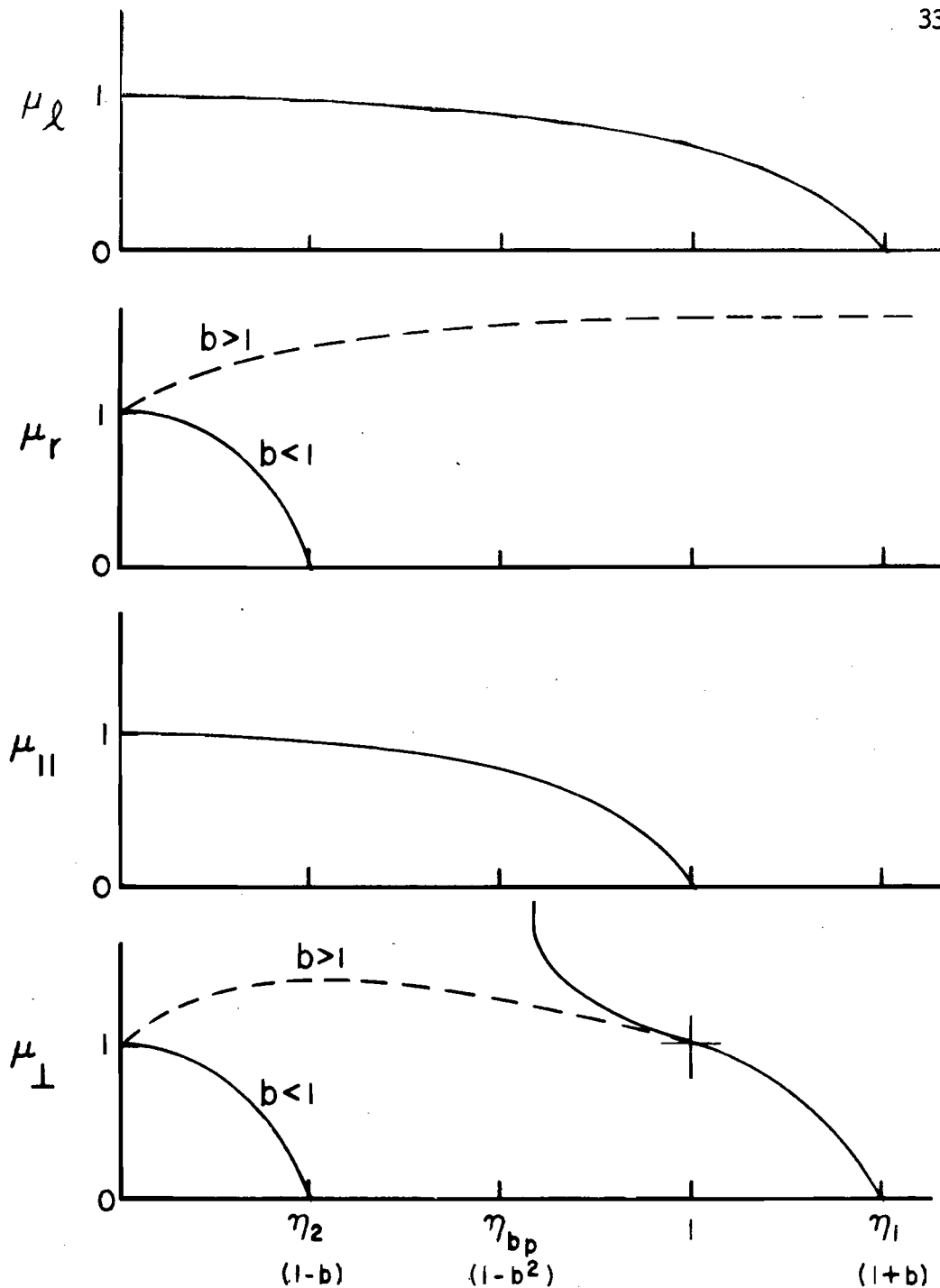
FIG. 2 QUALITATIVE VARIATION OF INDEX OF REFRACTION
WITH ELECTRON DENSITY FOR PROPAGATION
ALONG AND ACROSS MAGNETIC FIELD.

We note in passing that one can expect Cerenkov radiation under conditions where the phase velocity is very low, i. e., $\mu \rightarrow \infty$. [28] From Eq. (36) we obtain the "Cerenkov angle"

$$\tan^2 \theta_c = - \frac{\kappa_p}{\kappa_t}$$

(51)

$$= - \frac{(1 - \eta)(1 - b^2)}{1 - \eta - b^2}$$

in the absence of collisions.

F. Temperature and Ion Motion Effects

Two major simplifications have been implicit in the above discussion of high-frequency wave propagation, namely the neglect of the wave nature of the field (equivalent to the assumption of long wavelength or zero elec-tron temperature), and the neglect of ion motions (equivalent to the assump-tion of infinite ion mass). We now discuss these effects in turn.

In the absence of a magnetic field the conductivity is independent of the spatial variation (wave nature) of the perturbing electric field.[29] When a magnetic field is present, the electron gyration introduces a new scale of length, the gyroradius,

$$a = \frac{w_\perp}{\omega_b} = \sqrt{\frac{2kT}{m}} \; \frac{m}{eB} \; .$$

In magnetic fields of such strength that the gyroradius becomes as small as the mean-free-path, that is, for

$$\omega_b \gtrsim \nu$$

electrons are able to gyrate freely. If now the wave-length (in the plasma) of the perturbing electric field is comparable to the gyroradius

$$\frac{\lambda}{2\pi} \sim a \quad ,$$

the conductivity tensor can be expected to be significantly modified.[30]
These effects should not occur for

$$\frac{\lambda}{2\pi} >> a$$

or

$$\mu \cdot \frac{w_\perp}{c} \cdot \frac{\omega}{\omega_b} << 1$$

where μ is the index of refraction. At high temperatures (finite $w_\perp/c$) this inequality can be violated, especially at frequencies (generally near ω_b) for which μ is large.

The procedure which has been used to treat the high temperature case
is to solve the linearized Boltzmann equation assuming wave solutions varying
as exp ($\underset{\sim}{\gamma} \cdot \underset{\sim}{r}$ — i ω t). [30, 31, 32] Relativistic effects have so far been
neglected. Non-collisional attenuation due to phase mixing emerges in certain
regions and waves are found to propagate in some normally cutoff regions.
These effects become significant at temperatures of the order of a hundred
electron volts in the immediate vicinity of certain resonances (e. g., $\omega = \omega_b$).
They are generally important for the case (typical of pinch experiments)

$$\omega_p^2 >> \omega_b^2 \gtrsim \omega^2 \, ,$$

in which case the dielectric constant is modified by a term of the order of

$$1 + \beta \qquad\qquad (52)$$

where the ratio of material to magnetic pressure is $\beta = 2 \mu_o \, n \, k \, T / B^2$.
We note that β is a measure of the ratio of the gyroradius to the wave-
length of a free-space wave at the plasma frequency:

$$\frac{a}{(c/\omega_p)} = \left(\frac{w_\perp}{c}\right)\quad\left(\frac{\omega_p}{\omega_b}\right)$$

$$= \frac{1}{c}\sqrt{\frac{2kT}{m}}\;\sqrt{\frac{ne^2}{\epsilon_o m}}\quad\frac{m}{eB}$$

$$= \sqrt{\beta}.$$

(53)

The effects of ion motions have been neglected up to this point. The philosophy of computing the dielectric constant of a medium consisting of more than one component has been discussed by Darwin.[33] The inclusion of a finite ion mass is generally straightforward but algebraically tedious.[34]

Propagation characteristics of the plasma medium are considerably altered in the vicinity of the ion cyclotron frequency

$$\omega_{bi} = \frac{eB}{M}$$

and the hybrid frequency

$$\omega_{bh} = \frac{eB}{\sqrt{m\,M}}.$$

(54)

At high frequencies the special frequencies defined in Eqs. (41)

$$\omega_1 \quad \omega_2 \quad \omega_{bp} \quad \text{and} \quad \omega_p$$

are altered by correction terms of the order of $(1 + m/M)$. The simultaneous treatment of ion motions and finite temperature, but neglecting collisions, is contained implicitly in Bernstein's work. [32] As a limiting case at low frequencies one obtains the familiar d.c. dielectric constant perpendicular to a magnetic field [35]

$$\kappa = 1 + \frac{(m + M/Z)n}{\epsilon_o B^2} . \qquad (55)$$

G. Magnetic Permeability of a Magnetoplasma

Since the usual derivation of wave propagation in a material medium exhibits a dependence on the relative magnetic permeability, it is of interest to evaluate this effect in the case of a plasma. [35] The magnetic moment of an electron orbiting in a magnetic field is

$$p = \mu_o \, I \, A = \mu_o \left(- \frac{e \omega_b}{2\pi} \right) \left(\pi \frac{w_\perp^2}{\omega_b^2} \right) = - \mu_o \frac{e \, w_\perp^2}{2 \omega_b}$$

$$= - \mu_o \frac{\frac{1}{2} m \, w_\perp^2}{B}$$

where $w_\perp$ is the particle velocity. The magnetization (magnetic moment per unit volume) for a thermal distribution of electrons is

$$M = - \mu_o \ \frac{n \, k \, T}{B} \ .$$

The vector H is by definition

$$\mu_o \ H = \ B - M$$

$$= B + \mu_o \ \frac{n \, k \, T}{B} \ . \qquad (56)$$

Clearly no simple proportionality exists between H and B, and magnetic permeability is not a valid concept. Introducing the parameter

$$\beta \equiv \frac{2 \, \mu_o \ n \, k \, T}{B^2} \ , \qquad (57)$$

the ratio of material to magnetostatic pressure, we can write

$$M = - \tfrac{1}{2} \, \beta \, B,$$

$$\mu_o \ H = (1 + \tfrac{1}{2} \, \beta \ ) \ B, \qquad (58)$$

where, of course, β is an explicit function of B. When the plasma is immersed in a magnetostatic field strong compared with any wave fields, the relation between H and B yields a tangential relative permeability

$$\mu_t = \frac{1}{\mu_o} \frac{dB}{dH} = \frac{1}{1 - \frac{1}{2}\beta} \qquad (59)$$

In most experimental plasmas,

$$\beta << 1$$

so that the permeability is indistinguishable from unity. In the high temperature case as $\beta \rightarrow 1$ a number of effects enter and the problem must be treated from the point of view of particle dynamics rather than deducing separately the dielectric (inertial) and magnetic (thermal) effects.[30, 32] However we have already seen, from Eq. (52), that the proper calculations yield results, at least for certain regimes of parameters, which are of the order of Eq. (59). The extent to which this permeability model is useful in discussing high-temperature propagation has not yet been made clear.

H.   Propagation in Bounded Plasmas

The discussion so far has concerned propagation in a plasma of infinite extent. In the case of a plasma column[11, 12] or a plasma-filled waveguide[37] one is required to solve a boundary-value problem of some

complexity. The fact that the plasma is bounded leads, in general, to the existence of a.c. space charge at the boundary and in other regions of electron density gradients.[14] Further the action of the magnetic field couples together TE and TM modes which were independent in the case of isotropic media. Consider as an example the infinite-medium case of propagation along the magnetic field, in which the characteristic waves are circularly polarized. In the analogous waveguide case there can be no circularly polarized plane wave because of boundary conditions. In the so-called circularly-polarized TE_{11} mode, the fields at the center of the waveguide resemble a plane wave, but those near the walls are severly modified. Therefore wave propagation in the gyroelectric case becomes a complex matter.

While boundary problems of this type have been studied in great detail,[37] they often require information, on the size and profile of the plasma column and its location within the waveguide, which is not available in many experimental situations in controlled fusion work. At the same time so many parameters enter the problem that it is not practical to invert the analysis to obtain these secondary parameters from the observable quantities. We ask then under what conditions a plasma can be considered to be infinite, and the boundary effects neglected. Clearly this can be done for sufficiently short wavelengths (e.g., visible light). Since frequencies much in excess of the plasma frequency are uninteresting (the plasma having the r.f. properties of vacuum), we require

$$\frac{c}{\omega_p} << D \qquad\qquad (60)$$

where D is the dimension of the plasma (or scale length of gradients).
If this inequality is well satisfied the optical approach is most useful.
If the inequality is reversed, the problem must be approached from the
boundary-value point of view.[38] The large, highly-ionized plasmas of
controlled fusion research usually satisfy the inequality (60) .

III. TECHNIQUES FOR MEASUREMENT
OF PLASMA CONDUCTIVITY

A. Scaling Factors

We are here concerned with measurement of the electromagnetic properties of a plasma at high frequencies of the order of the plasma frequency. We are principally interested in the high-temperature case where collisions are generally negligible. Therefore, the conductivity depends almost entirely on electron density alone. There are two general approaches. First, one can obtain the real and imaginary components of the r. f. conductivity from the perturbations of the Q and resonant frequency of a cavity resonator. Secondly, one can measure the (complex) propagation constant of a traveling wave either in an "unbounded" plasma or a plasma-filled waveguide.

If the measurement is to sample the interior of the plasma, as is generally desired, the skin depth δ must be large compared to the plasma dimension D

$$\delta >> D,$$

where

$$\delta = \frac{1}{\operatorname{Im}\sqrt{\kappa}} \frac{c}{\omega}.$$

For the high-temperature, low-dissipation case, where $\nu/\omega_p << 1$, and in the absence of a magnetic field, for $\omega < \omega_p$

$$\delta = \frac{1}{[1 - (\frac{\omega_p}{\omega})^2]^{\frac{1}{2}}} \frac{c}{\omega} \qquad (61)$$

$$\overrightarrow{\omega << \omega_p} \quad \frac{c}{\omega_p},$$

44

and for $\omega^2 \gg \omega_p^2$,

$$\delta \doteq \frac{2\omega^2}{\nu \omega_p} \frac{c}{\omega_p} \ggg \frac{c}{\omega_p} \quad . \tag{62}$$

The transition at $\omega \approx \omega_p$ is very sharp (see Fig. 1). With a magnetic field, for propagation across the field with perpendicular polarization, from Eq. (44), for $\omega < \omega_1$

$$\delta = \left\{ \frac{\left[1 + (\frac{\omega_b}{\omega_p})^2 - (\frac{\omega}{\omega_p})^2 \right]}{\left[1 - (\frac{\omega}{\omega_1})^2 \right] \left[1 - (\frac{\omega}{\omega_2})^2 \right]} \right\}^{\frac{1}{2}} \frac{c}{\omega_p} \tag{63}$$

$$\xrightarrow{\omega \ll \omega_1} \left[1 + (\frac{\omega_b}{\omega_p})^2 \right]^{\frac{1}{2}} \frac{c}{\omega_p} \quad ,$$

where (see Eq. (41)) $\omega_{\frac{1}{2}} = \mp \frac{\omega_b}{2} + \left[(\frac{\omega_b}{2})^2 + \omega_p^2 \right]^{\frac{1}{2}} \quad .$

For $\omega_1 < \omega < (\omega_p^2 + \omega_b^2)^{\frac{1}{2}}$ and $\omega > \omega_2$

$$\delta \gg \frac{c}{\omega_p} \quad .$$

Note that in the parallel polarization case, with field, the field-free Eqs. (61, 62) apply. We thus distinguish two limits:

small plasma

$$D \ll \delta_o , \tag{64}$$

where δ_o is specified in the table, in which case the sample is fully penetrated by the wave at any frequency; and

large plasma

$$D >> \delta_o \tag{65}$$

in which case only certain frequencies ω_{test} can be used for interior sampling.

	No field or parallel polarization	Perpendicular polarization	
		$\omega_b < \omega_p \sqrt{2}$	$\omega_b > \omega_p / \sqrt{2}$
δ_o	$\dfrac{c}{\omega_p}$	$\left[1 + (\dfrac{\omega_b}{\omega_p})^2 \right]^{\frac{1}{2}} \dfrac{c}{\omega_p}$	
ω_{test}	$\omega > \omega_p$	$\omega > \omega_2$	$\omega_b > \omega > \omega_1$ or $\omega > \omega_2$

Since the transitions between cutoff and propagating bands are very sharp, the intermediate region between these two limits is small.

In the large plasma case, since frequencies of the order of the plasma frequency are to be used, it is possible to obtain by collimation spatial resolution to dimensions of the order of some few wavelengths (c/ω); i. e. , an optical approach is suggested. Conversely, in the small plasma case, for frequencies at or below the plasma frequency the wavelength is very large compared to the sample, and a lumped-sample model is appropriate.

We have not discussed the skin depth considerations for propagation along the magnetic field, which are somewhat different. In particular for the right-handed wave there is no cutoff if $\omega_b > \omega$. While longitudinal propagation is generally not applicable to stellarator and other toroidal geometries, it is clearly appropriate for magnetic mirror and other linear geometries. If the

discharge column is very long compared to its width, it is necessary to consider the problem as propagation in a plasma loaded waveguide.

B. Cavity Techniques

A well developed technique for measuring the conductivity of a plasma is to place the plasma in a suitable resonant cavity. The imaginary component of conductivity produces a change in resonant frequency, while the real component produces a change in Q. Since frequency shifts can be measured with extreme precision, the method is useful over a very wide range of electron densities. Most previous microwave studies of gas discharges have, therefore, used this technique.[39]

The technique is based on a perturbation formula for cavity frequency shift[40]

$$\frac{\Delta \omega}{\omega} = - \frac{1}{2 \omega \epsilon_o} \frac{\int \sigma_i E^2 d\tau}{\int E^2 d\tau} \tag{66}$$

where E is the microwave electric field and the integration is carried out over the cavity volume. This first-order formula is valid for the case

$$\omega^2 >> \omega_p^2 \ .$$

For the case of

$$\nu^2 << \omega^2$$

we have

$$\sigma_i = - \frac{n e^2}{m \omega} \left[\frac{1}{1 + (\nu/\omega)^2} \right] \approx - \frac{n e^2}{m \omega} \ .$$

Hence

$$\frac{\Delta \omega}{\omega} = \frac{e^2}{2 \epsilon_o m \omega^2} \ \bar{n} F \ , \tag{67}$$

where $\bar{n}$ is an average electron density and F is a shape function involving the spatial electron distribution and the cavity field configuration

The principal experimental problem is the design of the discharge geometry to permit reliable evaluation of the shape function F. Furthermore, since the size of a resonant cavity must be comparable with the wavelength, and the inequality $\omega^2 >> \omega_p^{\,2}$ must be maintained, there exists a limitation on the maximum electron density which can be measured for a given discharge size. In the usual case, to facilitate the evaluation of F, the plasma sample is taken to fill only a small portion of the cavity, which is resonant in a fairly low-order mode. This condition requires

$$D << d \sim \frac{2\pi c}{\omega}$$

where D and d are the dimensions of plasma and cavity, respectively. Together with the requirement $\omega^2 >> \omega_p^{\,2}$ this prescribes

$$\omega_p D << 2\pi c$$

which is essentially the same as the "small plasma" limit, Eq. (64). Note that the inequality can also be written

$$nD^2 << K \tag{68}$$

where K is a constant of the order of 10^{13} cm^{-1}.

The method can be extended by refining or avoiding the perturbation calculation,[41] or by the use of a high-radial-mode cavity.[42] As the "small plasma" limit is left behind, however, penetration (skin depth) effects must be considered.

An important feature of conductivity measurements with cavities (or any system involving standing waves) is that the system is relatively insensitive to plasma properties in regions of low electric field amplitude, whereas a running-wave system is equally sensitive everywhere. Thus good averaging over the sample volume is achieved only in the limits of very long or very short wavelength relative to the sample dimension.

C. Propagation Techniques

To study high-density discharges of arbitrary size and geometry one is generally forced to use microwave beams directed through the discharge by means of suitable antenna systems.[43, 44] This approach is particularly favorable to the case

$$\omega^2 >> \omega_p^2$$

$$\omega^2 >> (c/D)^2$$

where D is a dimension of the discharge. The first of these conditions permits convenient simplifications in the analysis by avoiding the plasma resonance, as in the cavity case; the second is essentially a diffraction condition which permits reducing the problem of propagation of a finite beam of electromagnetic waves through a finite plasma to a one-dimensional, plane-wave problem, as a first approximation. We note that the interrelationship of maximum measurable electron density and discharge size is quite different here from what we found for the resonant cavity technique, being particularly appropriate to the "large plasma" case.

It is basically a straightforward matter to measure the propagation constant of a microwave beam through a medium. The following simple applications to the case of high-temperature, highly-ionized plasmas (i.e., $\nu << \omega_p$) are obvious (see Fig. 3).

1. Simple transmission or reflection.

We have seen that for $n < n_c$ the plasma is transparent, and that for $n > n_c$ it is opaque and totally reflecting, where $n_c = (\epsilon_o m/e^2) \omega^2$ is the critical density. Furthermore, the transition between these conditions is very sharp. Thus in principal this elementary technique indicates whether a plasma is above or below the critical density. Measurement at a given frequency is capable of determining only one value of density. The sharpness of the transition implied by the sudden change in skin depth is not realized in practice because of the following factors:
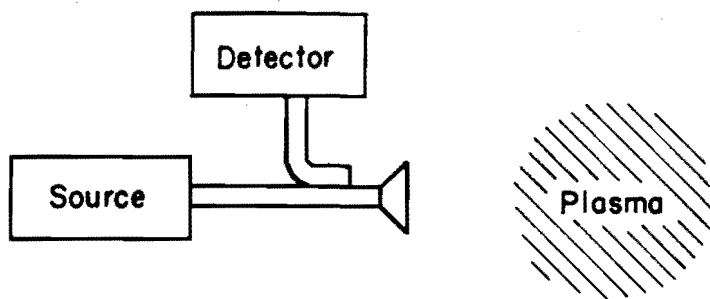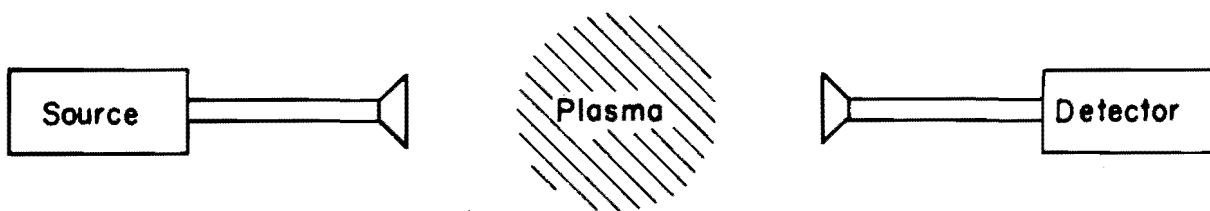
I. REFLECTION

2. TRANSMISSION
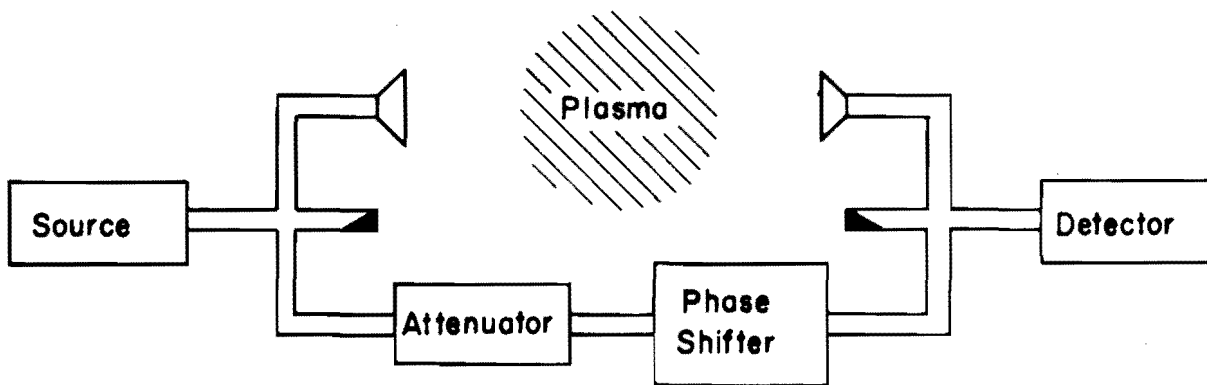
3. PHASE SHIFT

FIG. 3 MICROWAVE OBSERVATION SCHEMES

a.   For densities below but approaching critical, the dielectric constant discontinuity at the boundary produces an increasingly strong surface reflection (and corresponding reduction in transmission).

b.   If the plasma is only a few wavelengths thick, interference effects occur between the surface re-flections.

c.   Inhomogeneous density distributions are not averaged in a simple manner.

d.   Refraction and scattering by the plasma occur because of inadequacies in the one-dimensional, plane-wave approximation.

If the plasma is far above the critical density, an impinging signal is strongly reflected at the boundary. Therefore motions of the effective boundary pro-duce Doppler shifts in the frequency of the reflected signal.

2.   Phaseshift (microwave bridge or interferometer).

If the signal from an auxiliary transmission path, with adjustable ampli-tude and phase elements, is balanced against the primary transmission signal to give a null in the absence of plasma, the output signal of the waveguide (hybrid) junction is a measure of the attenuation and phaseshift in the primary path due to the plasma. In the fully transparent region of electron density, where $n << n_c$, a detected signal represents only phaseshift, which in turn is essentially a function of electron density only. Since the shift in phase can be calibrated, one has a continuous measurement of density between the upper limit of serious amplitude effects in the transmission path, and the lower limit of detector sen-sitivity. This technique is ideally suited to the observation of density as a function of time.

D. Simple Analysis of Phaseshift by a Plasma Slab

While most experimental situations approximate cylindrical symmetry, it is often possible to treat the plasma as a slab, reducing the problem to one dimension. One can further simplify the situation by assuming that plasma properties vary slowly near the boundaries so that reflection and interference effects are negligible.[45] This is usually known as an adiabatic approximation.

The phase constants for vacuum and plasma are, respectively,

$$\beta_o = \frac{2\pi}{\lambda}$$

$$\beta_p = \left[1 - \left(\frac{\omega_p}{\omega} \right)^2 \right]^{\frac{1}{2}} \frac{2\pi}{\lambda}$$

$$= \left[1 - \frac{n}{n_c} \right]^{\frac{1}{2}} \frac{2\pi}{\lambda} .$$

The phase advancement introduced by the plasma in a transmission path is then, in the adiabatic approximation,

$$\Delta \phi = - \int (\beta_p - \beta_o) \, dx$$

$$= \int \left\{ 1 - \left[1 - \frac{n(x)}{n_c} \right]^{\frac{1}{2}} \right\} \frac{2\pi}{\lambda} \, dx . \tag{69}$$

To first order in n/n_c, this becomes

$$\Delta \phi \approx \frac{\pi}{\lambda n_c} \int n(x) \, dx$$

$$= \frac{e^2}{2 \epsilon_o m c \omega} \int n(x) \, dx .$$

Thus for $n \ll n_c$ the phaseshift is linearly proportional to the electron density averaged along the propagation path. We can write

$$\bar{n} = \frac{\int_o^L n(x)\, dx}{L} = \frac{2\epsilon_o\, m\, c}{e^2}\; \frac{\omega\, \Delta\phi}{L} \left.\begin{array}{c}\\ \\ \\ \\ \\ \\ \end{array}\right\} (70)$$

$$\bar{n}\; [\,cm^{-3}] = 118.4\; \frac{f\,[\,cps\,]\; \Delta\phi\,[\,rad\,]}{L\,[\,cm\,]}\quad .$$

It is clear that in order to evaluate an electron density distribution from "free-space" phaseshift measurements we must know or assume two of the following three parameters:

1.   The shape function for the density distribution in space
along the transmission path (e. g. , rectangular, trapezoidal,
cosinusoidal, etc.);

2.   The index of width (thickness) of this shape function;

3.   The numerical density coefficient of the shape function.

In the first-order binomial expansion given above we are assuming from other considerations a characteristic thickness of the plasma; we then obtain a legitimate average electron density over this thickness. If however, we do not restrict our consideration to this first-order case, we can

1.   Expand the $\Delta\phi$ integrand to higher orders, in which
case the integrals obtained are successively higher moments
of the distribution function (e. g. , $\int n^2(x)\, dx$), or

2.   Integrate $\Delta\phi$ directly using an appropriate distribution
function.

In either case a meaningful average electron density is not obtained without an independent knowledge of the distribution function since the phaseshift is not linear with density, and the method becomes less useful for the quantitative measurement of even average densities. If, for example, one assumes a constant electron density (i. e. , a rectangular profile), which incidentally is somewhat contradictory to the adiabatic assumption, the integration is trivial and one obtains a parabolic dependence of density on phaseshift

$$\eta = \frac{n}{n_c} = 2\left(\frac{\lambda}{L}\, \frac{\Delta\phi}{2\pi}\right) - \left(\frac{\lambda}{L}\, \frac{\Delta\phi}{2\pi}\right)^2 \quad . \tag{71}$$

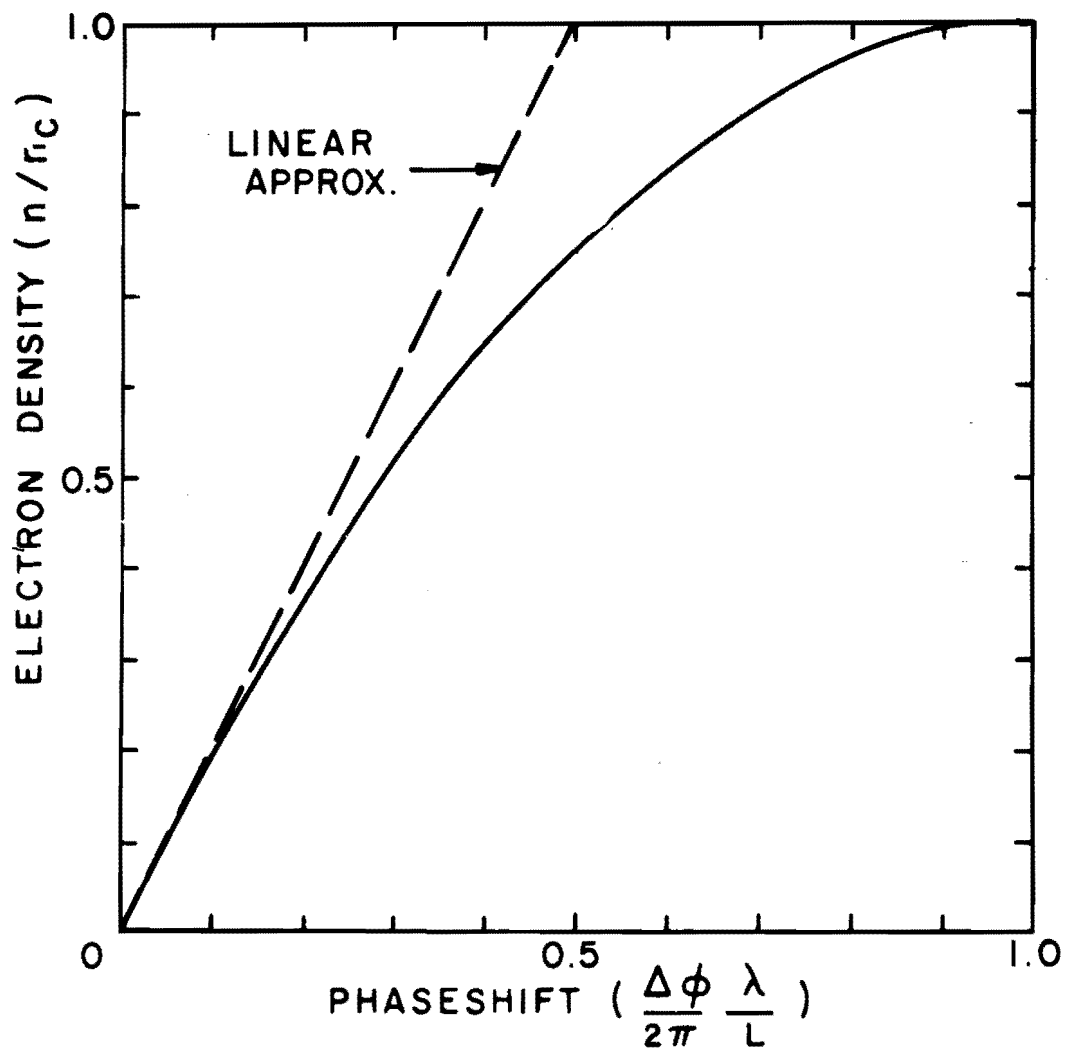Fig. 4 is a universal graph of this relation.

FIG. 4 UNIVERSAL DENSITY – PHASESHIFT
CURVE FOR PARALLEL POLARIZATION
AND UNIFORM DENSITY.

Returning to the first order approximation, we wish to evaluate the dynamic range of average densities which can be measured. Because of amplitude and non-linear effects,

$$n_{max} = \xi \, n_c = \xi \, \frac{\epsilon_o m \, \omega^2}{e^2} \qquad (72)$$

where ξ is a fraction which in a practical case might be 0.3. The minimum measurable density is

$$n_{min} = \frac{2 \epsilon_o m c}{e^2} \, \frac{\omega \psi}{L} \qquad (73)$$

where ψ is the minimum detectable phaseshift, which depends upon the detector noise level. Hence,

$$\frac{n_{max}}{n_{min}} = \pi \, \frac{\xi}{\psi} \, \frac{L}{\lambda} \sim \frac{1}{\psi} \, \frac{L}{\lambda} \, , \qquad (74)$$

The range of measurement scales with ω, while the maximum density scales with ω^2.

Finally we wish to discuss the serious limitations produced by finite size of the plasma and the failure of practical geometries to approximate the one-dimensional, plane-wave model. The typical geometry encountered in toroidal fusion devices is a cylindrical plasma with the microwave beam directed transverse to the discharge axis. In the frequency region for which the plasma is a dielectric the plasma acts like a diverging cylindrical lens, thereby influencing the amplitude of the transmitted signal. We have already mentioned interference effects on the transmitted amplitude which occur when the plasma is only a few wavelengths in diameter (thickness). These geometrical amplitude effects are troublesome because they obscure the dissipative absorption characteristic of the plasma itself.

A curved boundary increases the amount of energy reflected by surface discontinuities which does not re-enter the transmitting antenna. Depending

upon the nature and geometry of the material walls surrounding the discharge, it is possible for some of this scattered energy to reach the receiving antenna. If the microwave wavelength is comparable to the discharge diameter, diffraction and surface waves around the discharge are also possible. These effects introduce errors in the phase (and amplitude) of the resultant signal at the receiving antenna.

In the presence of a magnetostatic field, the problems introduced by a bounded microwave beam and plasma also include the fact that strictly speaking one cannot everywhere achieve the simple polarization case which does not couple to the magnetic field. Spurious effects can then occur when $\omega_b \approx \omega$.

E. Measurement of Density Profile

Since the phaseshift introduced by the plasma sample is in general a nonlinear function of electron density, one obtains information on the distribution of density (profile) by making simultaneous measurements at different frequencies and/or with different polarizations.

We can expand the integrand in Eq. (69)

$$\Delta\phi = \int_0^L \left\{ 1 - \left[1 - \left(\frac{\omega_p}{\omega}\right)^2 \right]^{\frac{1}{2}} \right\} \frac{2\pi}{\lambda} \, dx$$

$$= \int_0^L \left[\frac{1}{2} \frac{p\,n(x)}{\omega^2} + \frac{1}{8} \frac{p^2 n^2(x)}{\omega^4} \right. \tag{75}$$

$$\left. + \frac{1}{16} \frac{p^3 n^3(x)}{\omega^6} + \frac{5}{128} \frac{p^4 n^4(x)}{\omega^8} + \ldots \right] \frac{\omega}{c} \, dx \quad ,$$

where $p = e^2/\epsilon_o m$. Note that the series does not converge very rapidly. Consider two measurement frequencies

$$\omega_1 = \omega$$

$$\omega_2 = 2\omega$$

56

for which

$$\Delta\phi_1 = \frac{1}{2}\ \frac{p}{c\omega}\int n(x)\,dx + \frac{1}{8}\ \frac{p^2}{c\omega^3}\int n^2(x)\,dx$$

$$+ \frac{1}{16}\ \frac{p^3}{c\omega^3}\int n^3(x)\,dx + \cdots$$

$$\Delta\phi_2 = \frac{1}{4}\ \frac{p}{c\omega}\int n(x)\,dx\ \frac{1}{64}\ \frac{p^2}{c\omega^3}\int n^2(x)\,dx$$

$$+ \frac{1}{512}\ \frac{p}{c\omega^5}\int n^3(x)\,dx + \cdots$$

Therefore

$$\Delta\phi_1 - 2\Delta\phi_2 = \frac{3}{32}\ \frac{p^2}{c\omega^3}\int n^2(x)\,dx + \frac{15}{256}\ \frac{p^3}{c\omega^5}\int n^3(x)\,dx + \cdots \tag{76}$$

and we obtain for the first two moments of the distribution

$$\frac{p}{c\omega}\int n\,dx = 4\left\{\left[\Delta\phi_2 - \frac{1}{6}(\Delta\phi_1 - 2\Delta\phi_2)\right]\right.$$

$$\left. + \frac{1}{128}\ \frac{p^3}{c\omega^5}\int n^3\,dx + \cdots\right\} \tag{77}$$

$$\frac{p}{c\omega^3}\int n^2\,dx = \frac{32}{3}\left\{(\Delta\phi_1 - 2\Delta\phi_2) - \frac{15}{256}\ \frac{p^3}{c\omega^5}\int n^3\,dx - \cdots\right\} \tag{78}$$

The usefulness of this approach is limited by the accuracy of the differential measurement $\Delta\phi_1 - 2\Delta\phi_2$.

Procedures for obtaining profile information have been developed by Wharton and Slager and by Motley and Heald.[46] Wharton-Slager use only the magnetic-field-independent parallel-polarization case. Their data-reduction procedure is to calibrate the peak electron density by means of the cut-off of a "low-frequency" wave, and obtain profile information from the simultaneously observed phaseshift of a "high-frequency wave. Motley-Heald, using multiple polarizations, calibrate the average density with the "high-frequency" wave, infer profile from the "low-frequency" wave. Because of the greater phaseshift non-linearity of the perpendicularly polarized wave near cyclotron resonance, the multiple polarization technique is somewhat more sensitive. The W-S technique provides information only at the instants of time for which cut-off occurs; the M-H technique is limited to situations where the cyclotron frequency is comparable to the plasma frequency and is accurately known. Both methods benefit from additional phaseshift data-channels at other frequencies and/or polarizations, at the expense of instrumentation and data-reduction complexity. Neither method is able to distinguish a hollow discharge from a peaked one.

Another general approach to profile measurement is to observe reflection from the plasma at a frequency

$$\omega << (\omega_p)_{max.}$$

The position of the effective reflecting layer is close to the condition $\omega = \omega_p$, and therefore the profile can be mapped by measuring the reflecting depth as a function of frequency.[4] However, in practice, it is difficult to determine absolute position since mirrors a half wavelength apart produce the same reflection phase. In contrast to the ionospheric case, transit time (group velocity) measurements are not feasible. Furthermore the undertaking of reflection measurements on a transient discharge at more than one or two frequencies simultaneously leads to an unwieldy complexity of instrumentation. The measurement of the time variation of the position of the effective reflecting layer at one frequency is easily done in terms of the Doppler shift resulting from a moving mirror. This technique bears more on the observation of waves and perturbations on the plasma column than on the profile question.

In principal it appears that a measurement of amplitude and phase as a function of scattering angle (instead of just in the forward direction, i. e., "transmission") from a cylindrically symmetric plasma column should give information on profile. However the problems of (near-field) diffraction and propagation in inhomogeneous media inherent in this scheme make an analytical approach very formidable.

F. Microwave Phaseshift Display Circuits

For frequencies well above the plasma frequency a plasma is a low-loss transmitting medium the index of refraction of which is a function of electron density only. The index of refraction can be derived from the phaseshift of a transmitted wave. In general, microwave phase is measured by means of a bridge, in which the transmitted signal is added coherently to a reference signal of fixed phase. The optical analog is an interferometer of one sort or another. For plasma diagnostic purposes, we regard the microwave bridge and plasma transmission path as a transducer whereby a signal related to (average) electron density is displayed on an oscilloscope. The characteristics desired in phase-shift measuring systems for obtaining time varying density data, at a given fre-quency, are:

a. Wide density range.

b. Fast transient response.

c. Easily interpretable read-out.

d. Insensitivity to amplitude variations in transmitted signal from scattering and absorption as the plasma approaches critical density; and

f. Discrimination against plasma-generated noise of an amplitude comparable to the probing signal.

Figure 5 illustrates the basic microwave bridge circuit. The amplitude and phase controls in the reference path are adjusted so that the reference sig-nal interferes destructively with the transmitted signal, yielding a null output in the absence of plasma. For increasing density then the phase (and amplitude) unbalance produces an oscillatory output, shown in Fig. 5 for the case of a plasma thickness of approximately four wavelengths. At densities greater than
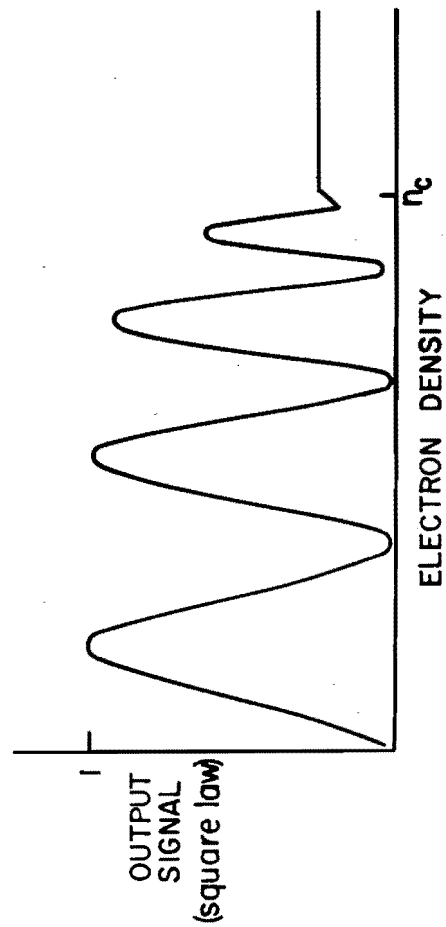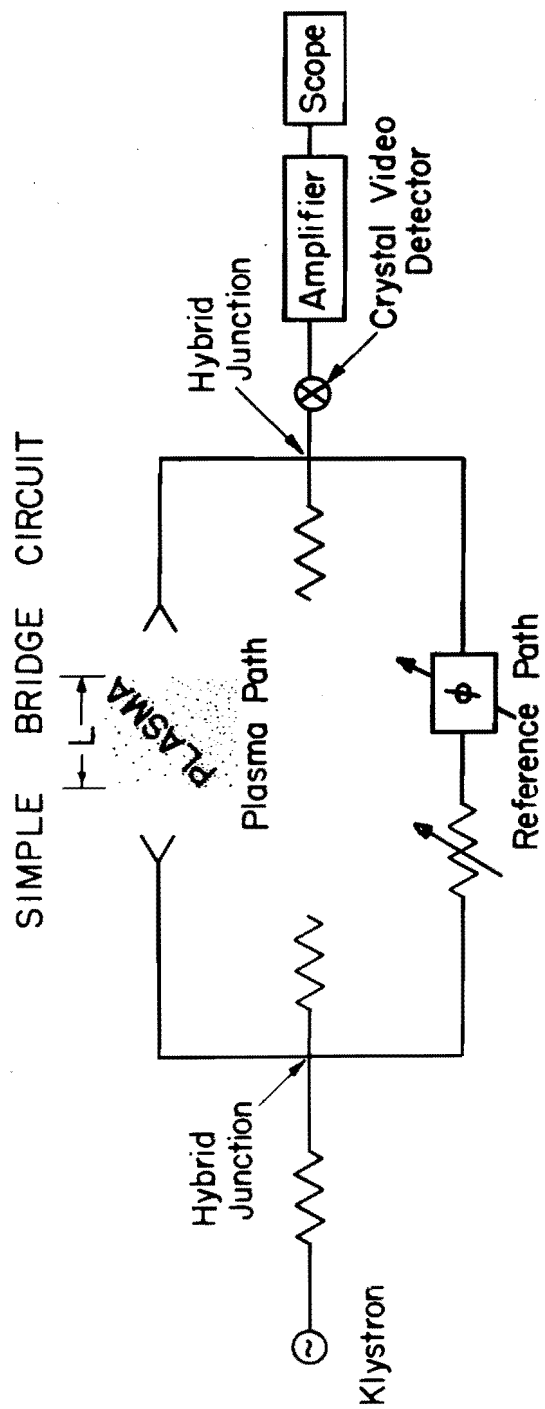
FIG. 5   A SIMPLE MICROWAVE BRIDGE FOR MEASURING THE PHASE
SHIFT PRODUCED BY A PLASMA, WITH THE RESPONSE OF THE
BRIDGE AS A FUNCTION OF ELECTRON DENSITY.

critical, the plasma signal is cut off. This is a simple, sensitive system. Its chief fault is that the multivalued dependence of density on output signal cannot be properly interpreted in the case of a transient discharge, the electron density of which is itself an oscillatory function of time.

Since under certain conditions phaseshift is linearly related to electron density, one would like a system which would present on an oscilloscope a pattern directly proportional to phaseshift, rather than being a sinusoidal function of phaseshift. The most widely used technique of this sort, developed by Gardner and Wharton at UCRL, produces horizontal stripes (or fringes) on the oscilloscope by means of an intensity-modulated raster.[43] The circuit is shown in Fig. 6. The deflection of the stripes is directly proportional to phase. The engineering design of this system has recently been discussed in some detail.[47]

For many instrumentation purposes it is desirable to have an output voltage proportional to phaseshift. A number of schemes for accomplishing this have been developed. Some employ feedback self-balancing bridges.[48, 49] Others use discriminator-integrator phase-modulation techniques.[48, 50] A major problem in systems of this type is the re-establishment of the correct phase indication after a period of time during which the plasma has been above critical density.

It is always possible to fold the bridge of Fig. 5 back on itself, placing a reflector behind the plasma and at the end of the reference path, and locating the detector on the fourth arm of the input hybrid junction. However, such a system is usually vulnerable to stray reflections both in the microwave components and in the plasma.

It is sometimes necessary to make density measurements in the presence of high-level, plasma-generated microwave noise. In extreme cases the first consideration is to protect the crystal from damage, by inserting as much resistive padding as is tolerable and by choosing the crystal operation point and load carefully. Passive bandpass filters and balanced detector arrangements, together with best use of the available signal power, minimize spurious signals in the bridge output.[47]
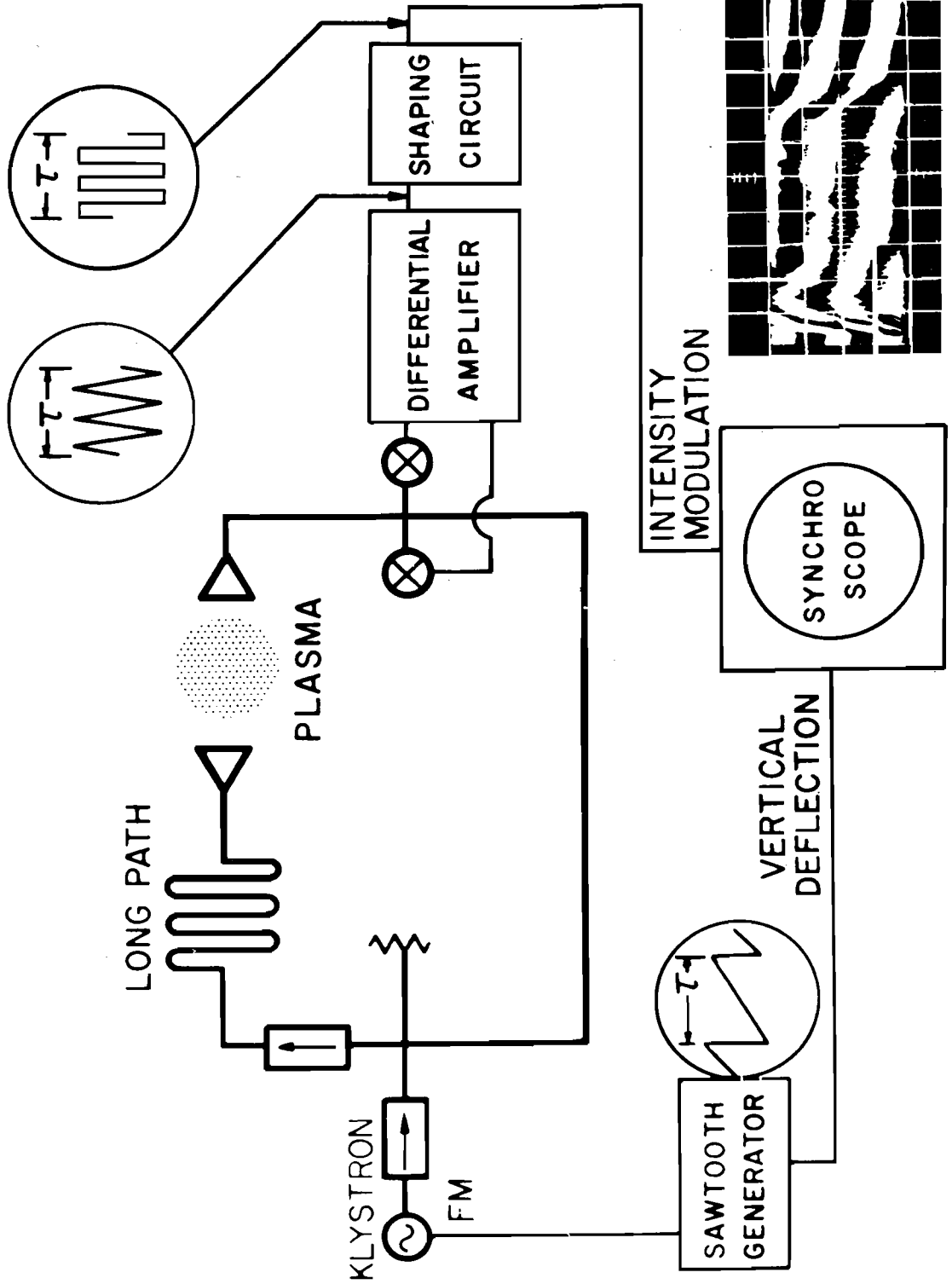
FIG. 6   Circuitry of the Gardner–Wharton interferometer, employing a highly-dispersive bridge and raster scope display.   The deflection of the bands, or "fringes", on the oscilloscope face is directly proportional to the phaseshift of the microwave beam transmitted through the plasma (Ref. 3).

G. The Geometrical Optics of Microwave Beams

The basic parameters of the microwave beam geometry are defined in Fig. 7. The problem is assumed two-dimensional, the elements being of infinite extent normal to the paper. If the plasma is distant by at least a wavelength from the antenna, induction effects can be neglected and the situation treated as a radiation problem. If

$$A/\lambda \gg 1$$

$$D/\lambda \gg 1 \,,$$

geometrical optics is a valid approximation and one can talk in terms of rays which, except for refraction, travel in straight lines.

We now consider the effect of refraction. Since the index of refraction of the plasma (no magnetic field, or parallel polarization) is

$$\mu = \sqrt{1 - \frac{n}{n_c}} < 1 \,,$$

the plasma column constitutes a divergent cylindrical lens. With the aid of Fig. 8 we compute the refraction of rays in the geometrical-optics limit for a homogeneous plasma with sharp boundaries. The exit angle θ_e is given in terms of the incident angle θ_i and the entrance ordinate $P/2$ by the following simultaneous equations:

$$\theta_e = \theta_i + 2(\theta_2 - \theta_1)$$

$$\sin(\theta_1 - \theta_i) = \frac{P}{D}$$ (79)

$$\sin \theta_1 = \mu \sin \theta_2 \,.$$

If now the exit ray is to strike the edge of the receiving aperture, at Cartesian coordinates $(R, A/2)$ with respect to the center of the cylinder cross section, we have the following condition on θ_i and $P/2$ for the most divergent ray

$$\mu = \sqrt{1 - \frac{n}{n_c}}$$

(a) ACTUAL GEOMETRY

(b) OPTICAL ANALOG

FIG. 7 MICROWAVE BEAM GEOMETRY.

FIG. 8 CYLINDRICAL REFRACTION
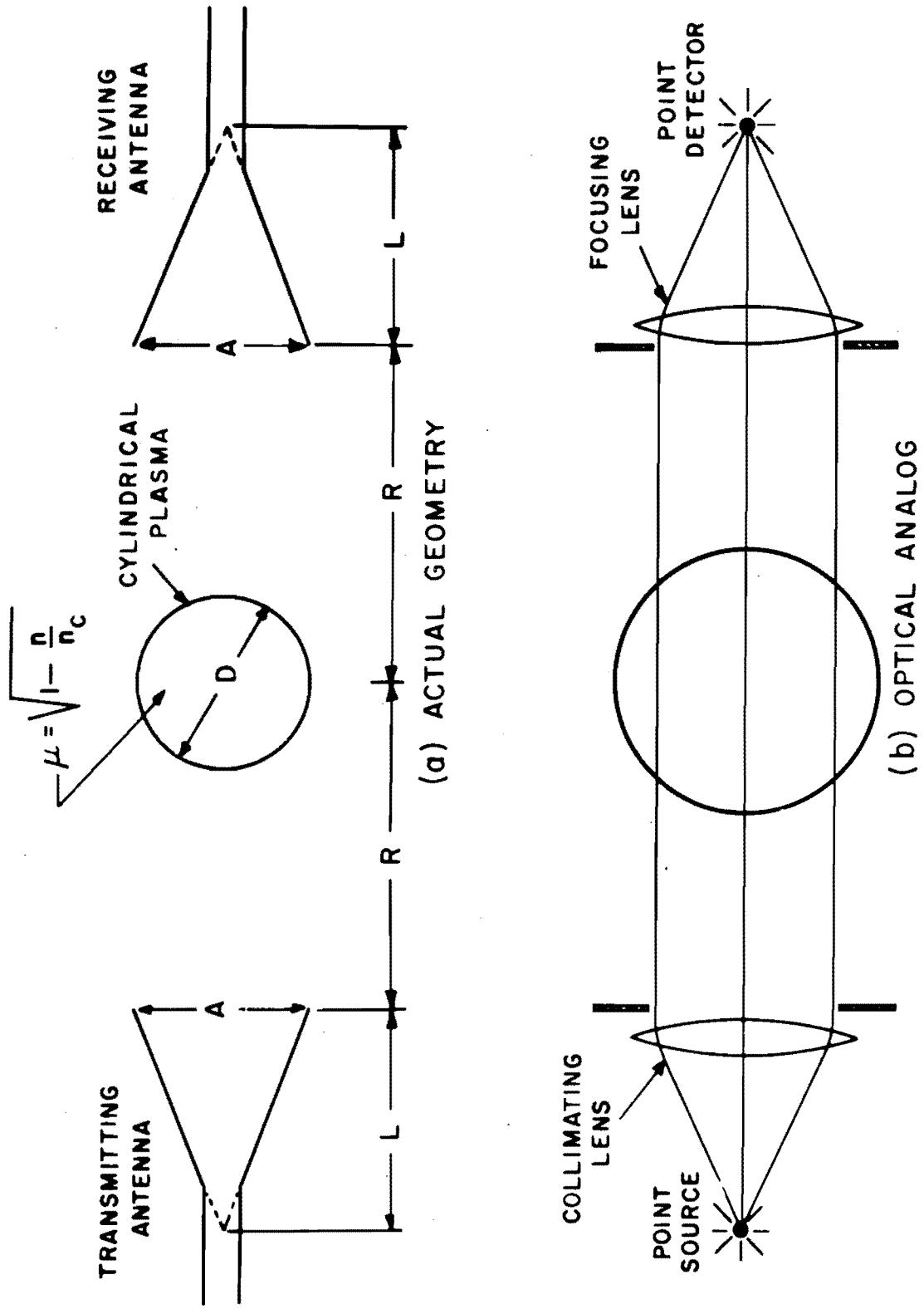
accepted by the receiving aperture:

$$\tan \theta_e = \frac{\frac{A}{2} - \frac{D}{2} \sin (\theta_i + 2\theta_2 - \theta_1)}{R - \frac{D}{2} \cos (\theta_i + 2\theta_2 - \theta_1)} \quad . \tag{80}$$

In many cases of practical interest it is reasonable to make small angle approximations. We obtain from Eq. (79)

$$\left.\begin{aligned}
\theta_1 &= \mu \theta_2 \\[2mm]
\theta_1 - \theta_i &= \frac{P}{D} \\[2mm]
\theta_e &= 2 \left(\frac{1}{\mu} - 1\right) \frac{P}{D} + \left[2 \left(\frac{1}{\mu} - 1\right) + 1 \right] \theta_i
\end{aligned}\right\} \tag{81}$$

and setting $m = \left(\frac{1}{\mu} - 1\right)$, from Eq. (80)

$$(2R - D) \left[2m \frac{P}{D} + (2m + 1) \theta_i \right]$$
$$= A - D \left[(2m + 1) \frac{P}{D} + 2(m + 1) \theta_i \right] . \tag{82}$$

Solving for P/D, we have

$$\frac{P}{D} = \frac{A - \left[2 (2m + 1) R + D \right] \theta_i}{4m R + D} \quad . \tag{83}$$

For $\mu < 1$ the largest angle involved is $\theta_i + 2\theta_2 - \theta_1$, and the small angle approximation is self-consistent for

$$(2m + 1) \frac{P}{D} + 2(m + 1) \theta_i \ll 1 \tag{84}$$

or

$$\frac{P}{D} << \frac{1 - 2(m + 1)\theta_i}{2m + 1} \quad . \tag{85}$$

In the geometrical optics limit, with a point source at $-(L + R)$, we have from Fig. 9

$$\sin \theta_i = \frac{P}{2(L + R) - D \cos(\theta_1 - \theta_i)} \tag{86}$$

or for small angles

$$\theta_i \approx \frac{P}{2(L + R) - D} \quad . \tag{87}$$

Eliminating θ_i in Eq. (83), we have

$$\frac{P}{D} = \frac{A}{4mR + D + \dfrac{2(2m + 1)RD}{2(L + R) - D} + \dfrac{D^2}{2(L + R) - D}}$$

$$= \frac{A[(L + R) - D/2]}{4mR(L + R) + D(L + 2R)} \quad . \tag{88}$$

We recall that $P/2$ is the largest entrance ordinate of rays which pass into the receiving aperture. Therefore, when $P/D << 1$ the cylinder is equivalent to a slab of thickness D. With the above evaluation of θ_i the small angle approximations will be self-consistent if from Eq. (85)

$$\frac{P}{D} << \frac{2(L + R) - D}{2(2m + 1)(L + R) + D} \tag{89}$$

or using Eq. (88)

$$A << \frac{4mR(L + R) + D(L + 2R)}{(2m + 1)(L + R) + D/2} \quad . \tag{90}$$

UNREFRACTED RAY

REFRACTED RAY

A

P

D
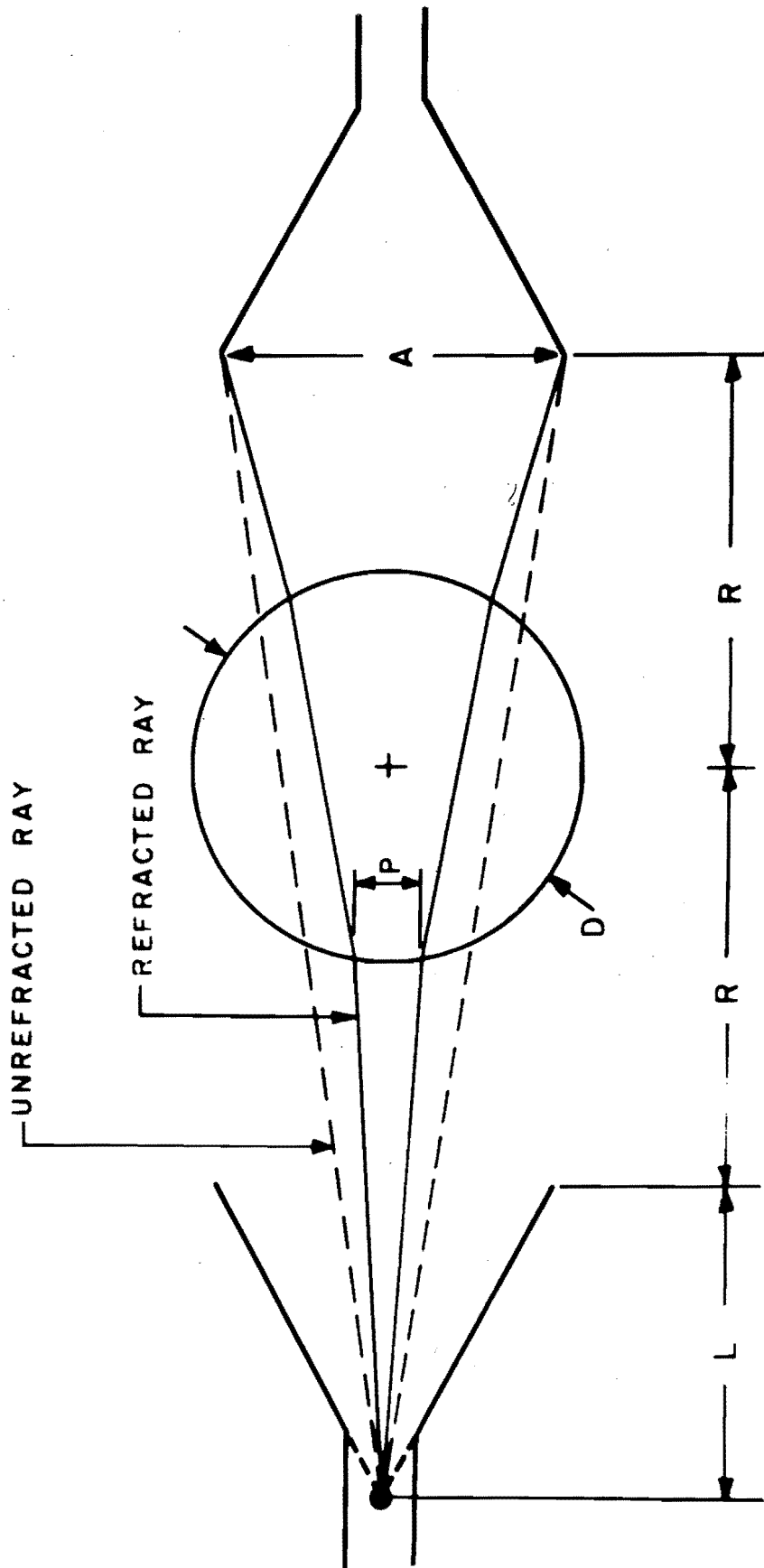
R

R

R

L

FIG. 9   EFFECT   OF   REFRACTION   IN   GEOMETRICAL

OPTICS   APPROXIMATION.

Neglecting dissipation in the plasma, we obtain a reduction in amplitude at the receiving aperture because of the loss of highly refracted rays. This (power) transmission ratio is

$$\frac{P}{P\,(\mu = 1)} = \frac{D\,(L + 2R)}{4m\,R\,(L + R) + D\,(L + 2R)} \tag{91}$$

where we recall that

$$m = \frac{1}{\mu} - 1 = \frac{1}{\sqrt{1 - \frac{n}{n_c}}} - 1 \approx \frac{1}{2}\,\frac{n}{n_c} + O\,\left(\frac{n}{n_c}\right)^2 \ .$$

Fig. 10 shows this transmission loss as a function of electron density for the particular case of

$$\frac{4\,R\,(L + R)}{D\,(L + 2\,R)} = 3.6\ .$$

For comparison we compute the dissipative loss in the plasma due to collisions. For $n < n_c$ and low dissipation (i. e., $\omega^2 > \omega_p^2 >> \nu^2$) this is given in decibels by

$$- 8.686\,\alpha\,D = \pi\,(8.686)\,\frac{\frac{n}{n_c}}{\sqrt{1 - \frac{n}{n_c}}}\,\frac{\nu D}{2\pi c}\ , \tag{92}$$

for rays passing near the center of the plasma. Fig. 10 shows this relation for the numerical case

$$\frac{\nu D}{2\pi c} = \frac{\nu}{\omega}\,\frac{D}{\lambda} = 0.1\ .$$

We next consider the question of interference effects due to reflections at the sharp plasma-vacuum interfaces. In the usual case of $P/D << 1$ the only rays received are those which pass near the center of the plasma and we can regard the plasma as a slab of thickness D. For the case of thin (lossless) slabs Stratton gives as the power transmission coefficient[45]
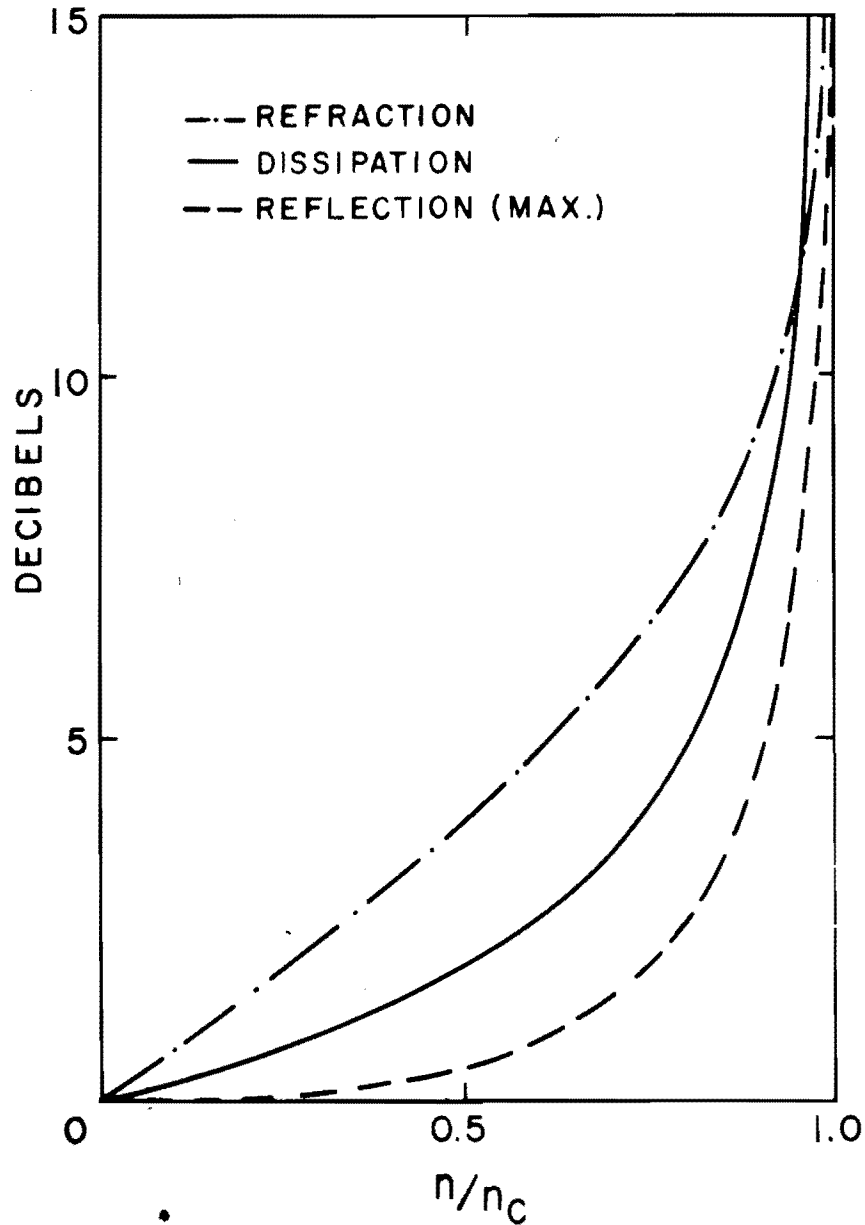
FIG. 10 LOSS OF TRANSMITTED AMPLITUDE FROM REFRACTION $\left[\frac{4R(L+R)}{D(L+2R)} = 3.6 \right]$, DISSIPATION $\left(\frac{\nu D}{\omega \lambda} = 0.1 \right)$, AND REFLECTION.

$$T = \frac{1}{1 + (\frac{1 - \mu^2}{2\mu})^2 \sin^2 (2\pi \frac{\mu D}{\lambda})} \tag{93}$$

which varies between

$$(\frac{2\mu}{1 - \mu^2})^2 < T < 1$$

as the relative phasing of the reflections changes.* This maximum transmission loss is also shown in Fig. 10.

---

* We note, in passing, a convenient procedure for calculating the maximum transmission loss due to reflection. The voltage standing-wave ratio of a single discontinuity is the relative index of refraction μ (or $1/\mu$, whichever is greater than unity). From standard transmission-line theory the maximum VSWR from two such discontinuities is the product of the respective VSWR's (and the minimum, the quotient). Thus the maximum transmission loss due to reflection from a slab can be obtained from standard graphs[50] assuming a single discontinuity

$$VSWR = \begin{cases} \frac{1}{\mu^2} & \mu < 1 \\ \\ \mu^2 & \mu > 1 \end{cases}$$

This procedure applies only if there is no dissipative loss between discontinuities.

H. Diffraction Considerations

We now review some of the basic principles of diffraction. Consider a slit of width A and an observation point P centrally located a distance R away. The slit is illuminated by plane waves incident from the left. We wish to investigate the nature of the radiation field in the vicinity of P.
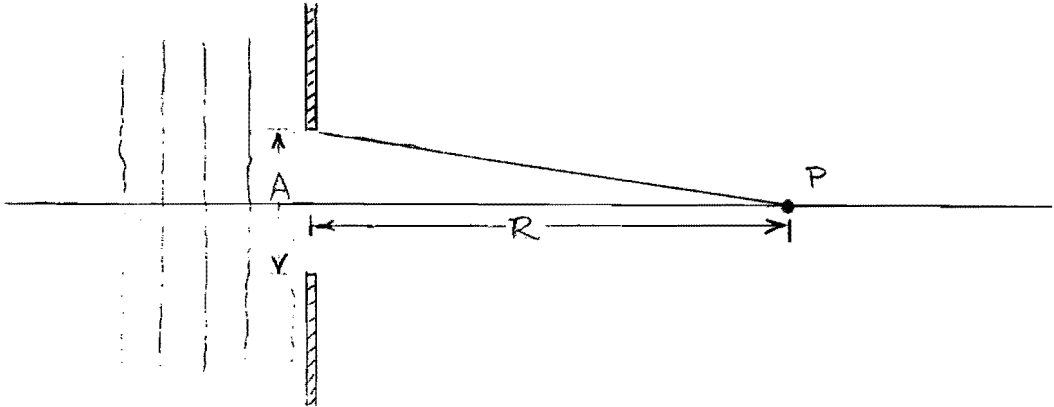
The width of the slit can be characterized by the number n of Fresnel half-period zones which it subtends at the point P; thus

$$(\frac{A}{2})^2 + R^2 = (R + \frac{n}{\lambda})^2$$

from which we obtain

$$R = \frac{A^2 - n^2\lambda^2}{4n\lambda}$$
$$n = \frac{2R}{\lambda} \left\{ \left[1 + (\frac{A}{2R})^2 \right]^{\frac{1}{2}} - 1 \right\} . \tag{94}$$

We will be concerned only with cases where induction fields can be neglected and therefore

$$R \gtrsim \lambda ,$$

which requires

$$A \gtrsim \sqrt{n(n+4)\lambda} . \tag{95}$$

If A, R, and λ are such that n is of the order of one to ten, then strong interference fluctuations are to be expected in the spatial vicinity of the point P. The distance between peaks and valleys, in fractions of a wavelength, can be estimated from

$$\frac{1}{\lambda} \ \left| \ \frac{dR}{dn} \ \right| = \frac{1}{4} \left[\ 1 + \left(\frac{A}{n\lambda}\right)^2 \ \right] \tag{96}$$

which, excluding induction fields, is

$$\gtrsim \frac{1}{2} + \frac{1}{n} \ .$$

For low-order Fresnel interference effects the amplitude variations are very large, the field pattern is "choppy", and phase anomalies occur.[52, 53]

If n is very large, our exclusion of induction-field effects requires

$$A \gtrsim n\lambda >> \lambda \ ,$$

and the intensity distribution near P is essentially that of geometrical optics; i. e. , uniform intensity falling sharply to zero in the geometrical shadow of the aperture. The relative variation in amplitude, although of periodicity λ , is small. If a lens of focal length R is inserted at the slit a Fraunhofer diffraction pattern is obtained in the plane containing P , as in the familiar problem of the astronomical telescope.

If, on the other hand, n is much less than unity, a Fraunhofer diffraction pattern is obtained at P even without a lens. This is the familiar far-field case of conventional microwave antenna theory. To the extent that

$$n \approx \frac{A^2}{4\lambda R} << 1$$

we have

$$R >> \frac{A^2}{4\lambda}$$

This is equivalent to the well-known rule for the far (Fraunhofer) field of an antenna, which is usually written[*]

$$R \gtrsim \frac{A^2}{\lambda} \tag{97}$$

and signifies that the maximum phase differential between "rays" is less than $\lambda/8$, or that the aperture is less than one-fourth of the first Fresnel half-period zone.[54] The total angular width of the central maximum of the Fraunhofer diffraction pattern is $2\lambda/A$. Therefore the spatial width of the central maximum falling on a plane in the far field is

$$\frac{2\lambda}{A} R \gtrsim 2A.$$

Thus if $A \gtrsim \lambda$ the intensity distribution in the vicinity of P is quite smooth over distances of the order of a wavelength, as in the high n case but in contrast to the $1 \lesssim n \lesssim 10$ case.

The behavior of the field can be expected to be qualitatively like the far-field up to a range corresponding to the first Fresnel half-period zone[55]

$$R = \frac{A^2}{4\lambda} .$$

The far-field region can be effectively extended somewhat closer to the antenna aperture by the use of a lens to partially overcome the diffraction spreading.[56] The angular half-width of the central maximum of the Fraunhofer diffraction pattern is λ/A. On geometrical optics a ray leaving the edge of an aperture of width A at this angle appears to originate at a point located a distance $A^2/2\lambda$ on the source side of the aperture, and therefore the insertion of a lens of focal length $F = A^2/2\lambda$ will render this extreme ray parallel to the axis. The so-called "f/-number" of such a lens is

$$"f/" = \frac{F}{A} = \frac{A}{2\lambda} .$$

_____

[*] Some antenna engineers use the criterion $R \geq 2A^2/\lambda$, corresponding to $\lambda/16$ or one-eighth zone. Amplitude errors due to interference are then about 2% as opposed to 5% for the criterion given above.

It is an interesting property of microwave optics that one can satisfy the Fraun-hofer diffraction criterion $R \gtrsim A^2/\lambda$ without the use of collimating lenses as required in the optical region. That is, the "far field" of a radiation aperture or an obstacle, is a much closer distance, in wavelengths, than for similar apertures in the optical case. Therefore in many situations far-field theory can be used to describe the microwave field. Meanwhile the use of lenses be-comes less powerful since the focal length F of the lens must be

$$F \lesssim \frac{A^2}{\lambda}$$

if the focusing effect of the lens is to influence the diffraction pattern appreciably. The "f/-number" is then

$$"f/" \lesssim \frac{A}{\lambda} \quad .$$

When the geometrical optics condition $A/\lambda >> 1$ no longer holds, lens designs of small "f/-number" are called for which show strong aberation and are other-wise impractical. Stated differently, the width of the (Fraunhofer) diffraction pattern at the focus of a lens is

$$\frac{2\lambda}{A} F = 2 "f/" \lambda \gtrsim \lambda \quad .$$

We can thus prepare the following table summarizing the characteristics of the radiation field for various regimes of the parameters

	$\frac{A}{\lambda} \sim 1$	$\frac{A}{\lambda} >> 1$
$n >> 10$	induction field region	normal geometrical ray optics (collimation $\sim A$ without lens; $\sim \lambda$ with lens)
$1 \lesssim n \lesssim 10$		Fresnel interference, "choppy" intensity distribution (collimation $\sim A$)
$n << 1$	Fraunhofer diffraction radiation pattern (collimation $\frac{2\lambda R}{A} \gtrsim A$)	

The best collimation $(\sim \lambda)$ is obtained in the $A/\lambda \sim 1$, $n \ll 1$ case (antenna far-field) and the $A/\lambda \gg 1$, $n \gg 10$ case with lens (geometrical optics). The latter however is a strongly converging wave passing through a focus.

Diffraction enters the plasma probing problem in two aspects. One is the nature of the radiation field at the position of the plasma and the receiving antenna produced by the transmitting antenna. The other is the diffraction of the transmitted radiation by the plasma column itself. In the low-order Fresnel region of an antenna the field pattern is characterized by strong amplitude variations and phase errors.[53, 57] It appears best to design the experiment so as to avoid this region. If n, the number of Fresnel zones, is either very large or small throughout the space occupied by plasma and receiving antenna, then the illumination will be fairly uniform.

Diffraction (scattering) of a plane wave by a homogenous, isotropic, cylindrically-symmetric plasma can be treated exactly by a boundary-value calculation.[12, 58] Unless simplifying approximations can be made,[59] numerical calculations for given experimental situations are usually difficult to carry out, even with computers, since extensive summations over Bessel functions must be performed for each point. Calculation is especially difficult when D/λ is not much larger than unity, and when the receiving antenna is at a finite distance and subtends a non-zero angle at the plasma axis. The effect of a density profile is difficult to handle since the boundary problem can no longer be solved exactly. Scattering from an anisotropic object (plasma in a magnetic field) is also difficult to analyze.[60] Interference between reflections of plasma and antenna system add another complication.[61] In the face of theoretical difficulties one approach is to study near-field problems empirically, using simulated geometries of known properties.[62, 63]

I. Optimization of Antennas

We assume that we are given the diameter D of a cylindrical plasma column and the wavelength λ with which we are to probe it. We assume that λ, determined by the electron density range to be measured and the availability of short-wavelength instrumentation, is small compared to D but by no means negligible. Since we wish to obtain a reasonable average of the electron density independent of refraction (and diffraction) by the plasma, we wish to achieve

the maximum possible collimation of the microwave beam so that it effectively passes along a diameter. We have seen from a geometrical optics point of view that when $\mu < 1$ the divergent lens action improves the effective collimation by refracting non-diametric rays out of the receiving aperture. However because of the danger of reflection from such extraneous obstacles as the vacuum system walls, and because of the desire to conserve feeble millimeter-wave power, we wish to maximize the power in received diametric rays and minimize it in non-received and/or non-diametric rays. That is we wish to minimize the insertion loss between antennas while ensuring that most of the radiation passes close to the axis of the plasma.

The most clear cut situation is

$$D >> A >> \lambda$$

which conforms closely to infinite-slab, geometrical-optics conditions. However our interest is in the case where

$$1 \lesssim \frac{D}{\lambda} \lesssim 10 \ .$$

If $A > D$, appreciable energy passes around the plasma, reducing sensitivity and severely complicating interpretation. With

$$D \gtrsim A \gtrsim \lambda \ ,$$

in order to avoid induction field effects and Fresnel-zone interference effects, we must have the plasma located in the far-field of the antennas, $R \gtrsim A^2/\lambda$.

It is a well-known rule of antenna engineering that for a pair of antennas to be located in the far-field region, by the usual A^2/λ criterion, the minimum insertion loss is of the order of 16 db.[54] Since only about two percent of the radiated power is received, the probability of interference from spurious reflected signals is high. We are therefore interested in pushing as close to the near field (Fresnel zone number $n \gtrsim 1$) as possible without encountering severe amplitude and phase disturbances from interference. This leads to the alternative of small (non-directive) antennas relatively close to the plasma or

large (directive) antennas farther back.

The concentration of r. f. energy produced in the field of a horn antenna depends upon two factors, the width of the wavepacket launched and the angle of spread of the wave. Empirical plots of intensity contours in the field of millimeter horn antennas indicate that one-half of the energy is confined within a beamwidth[64].

$$W = \left[\left(\frac{aA}{2} \right)^2 + \left(\frac{b\lambda R}{A} \right)^2 \right]^{\frac{1}{2}} \tag{98}$$

where a and b are correction factors depending on the specific geometry and departing only slightly from unity. For a given λ and R this is minimized when

$$A = \sqrt{\frac{2b}{a} \lambda R} \tag{99}$$

giving

$$R = \frac{a}{2b} \frac{A^2}{\lambda} \tag{100}$$

$$W_{min} = \sqrt{ab\lambda R} .$$

We note that this condition corresponds to an aperture of one-half a Fresnel half-period zone at R. The insertion loss between two such antennas spaced 2R apart is about 8 db, depending upon the other dimension of the antenna aperture. We now consider the role of the diameter D of the plasma column. The relative beam size W/D varies as $\sqrt{R}/D$, whereas the relative spreading of the field over the plasma

$$\frac{D}{W} \left(\frac{\partial W}{\partial R} \right)_{W_{min}}$$

varies as D/R. Since we wish

$$W << D << R$$

we arbitrarily take

$$D = \sqrt{W_{min} R} = (ab\lambda R^3)^{\frac{1}{4}} .$$

(101)

Recapitulating, given D and λ and assuming $a = b = 1$, we choose

$$R = (\frac{D}{\lambda})^{1/3} D$$

(102)

$$A = (2\lambda R)^{\frac{1}{2}} = \sqrt{2} (\frac{\lambda}{D})^{1/3} D.$$

This heuristic argument is founded on the vague assumption that there is some virtue in minimizing the beamwidth at the plasma by choice of A and then compromising in the choice of R such that

$$\frac{D}{W_{min}} = \frac{R}{D} .$$

The effect is to prescribe a situation in which the plasma is located slightly inside the conventional far-field boundary. We have seen however that under these conditions diffraction anomalies should not be very severe. Note that when $D/\lambda >> 1$, $R << D^2/\lambda$, and therefore the plasma approximates an infinite slab as far as diffraction is concerned.

Empirical measurements by Barbara Rosen, in which a homogeneous plasma is simulated by a hole cut in a solid dielectric in which the antennas are imbedded, have shown that in a geometry similar to that given by the above prescription a plane-wave, infinite-slab analysis is reasonably accurate for $D/\lambda \gtrsim 3$, and that no serious effects arising from diffraction and interference can be observed.[62]

The preceding discussion has been based on the assumption of simple horn antennas without lenses.[65] If a horn is "long" $(L \gtrsim A^2/\lambda)$ its far-field pattern cannot be narrowed by addition of a lens. However, in an earlier
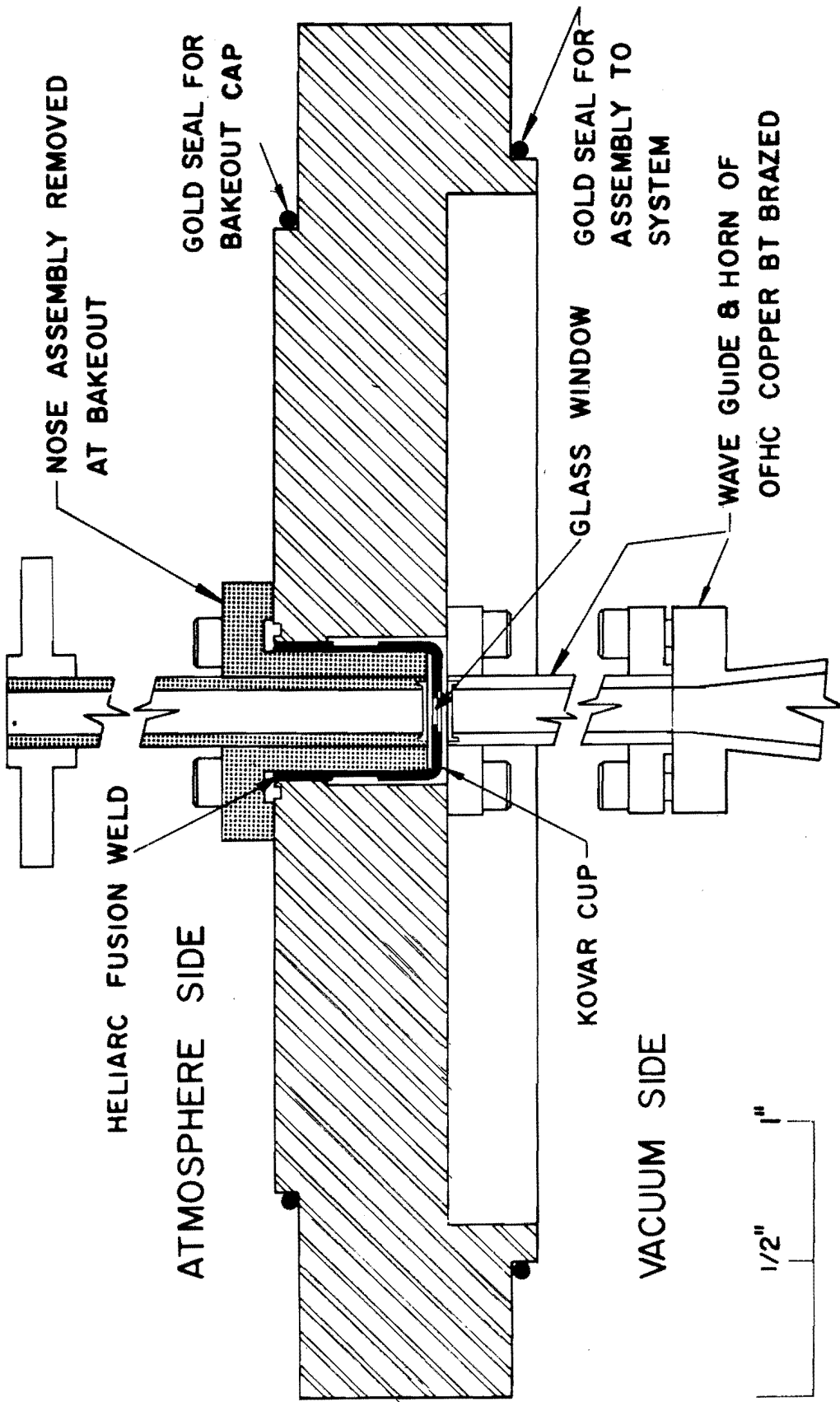
section we have discussed the use of a lens to focus the energy at a distance $R \lesssim A^2/\lambda$. The suggestion has been made to use converging lenses focused at the plasma axis.[66] This is chiefly based upon the geometrical-optics argument that all rays pass diametrically through the plasma, thereby removing the refraction and sampling difficulties of the "plane-wave" approach. If $A/\lambda \gg 1$ so that a good focus can be obtained, and if this focus ($\sim \lambda$) is small relative to the plasma, $D/\lambda \gg 1$ — that is, a good geometrical optics situation — this procedure may have merits. However, in this case the relative r.f. field strength becomes very high in the vicinity of the focus, so that nonlinearities in the r.f. properties of the plasma may be troublesome.[17] If on the other hand $D/\lambda \sim 1$, phase anomalies in the vicinity of the focus could severely complicate the interpretation.[53] In this case it appears that if lenses are to be used at all they should be focused at the opposite antenna or beyond.[56]

Because of the perturbation which thick dielectric windows (glass, quartz, etc.) make on the field of a millimeter-wave antenna,[61] it is customary to locate the vacuum seal at a convenient point back in the waveguide so that the antennas are wholly within the vacuum system. Such window design follows standard practice as used in microwave tube output windows and waveguide pressurizing windows.[67] Figure 11 shows the basic design of the window assembly which has been found highly satisfactory in baked ultra high-vacuum equipment.[68]

J. Density Profile Effects

When a plasma sample is homogeneous, as has been generally assumed in the above discussions of microwave optics, boundary value problems can be solved in many simple geometries.[12, 45, 58] However, it is to be expected that an experimental plasma will not be strictly homogeneous. Indeed the electron density profile is generally not known a priori and must be regarded as a parameter to be determined experimentally. In the opposite extreme of very slowly varying propagation characteristics,

$$\frac{\lambda}{\kappa} \, |\nabla \kappa| \ll 1,$$

80

NOSE ASSEMBLY REMOVED AT BAKEOUT

GOLD SEAL FOR BAKEOUT CAP

GOLD SEAL FOR ASSEMBLY TO SYSTEM

GLASS WINDOW

WAVE GUIDE & HORN OF OFHC COPPER BT BRAZED

HELIARC FUSION WELD

ATMOSPHERE SIDE

KOVAR CUP

VACUUM SIDE

1/2" 1"

70 kmc MICROWAVE WINDOW ASSEMBLY

FIG. II

the adiabatic approximation, analogous to the WKB approximation in quantum mechanics, is appropriate and the procedure mentioned above for calculating phaseshifts,

$$\Delta\phi = \int_L [u(x) - 1] \frac{2\pi}{\lambda} dx ,$$

is fully valid. Refraction can be treated in the adiabatic approximation for the cylindrically (or spherically) symmetric case.[69]

The intermediate case, where the propagation constants are neither sharply discontinuous nor slowly varying, is difficult to treat except in special cases.[70] Clearly discontinuity interference effects, leading to reflection and to perturbations on the transmitted amplitude and phase, will be less in the inhomogeneous than in the homogeneous case.[45] Diffraction effects are difficult to study analytically in the intermediate inhomogeneity case.

K. "Doppler Radar" Measurements

When the probing frequency is below the plasma frequency corresponding to the maximum electron density, the incident wave is strongly reflected. If the reflection layer (i. e., where $\omega \approx \omega_p$) is moving, due for instance to translation or contraction of the discharge column, the reflected wave is Doppler shifted. For normal incidence the shift is

$$\frac{\Delta\omega}{\omega} = \frac{2\beta}{1-\beta} \approx 2\beta$$

where $\beta = v/c$ and v is the velocity of the moving mirror in the direction of the transmitter. The use of a frequency-modulation receiver in the circuit of Fig. 12 is straightforward. By integrating the discriminated output signal, which is proportional to velocity, one obtains a signal proportional to the time-varying position of the reflecting layer. This technique is useful for observing relatively low-frequency (megacycle) oscillations in plasma density and position. The signals can easily be interpreted quantitatively if the discriminator and integrator characteristics are known. This procedure is valid so long as the density gradient is steep enough that the relative phaseshift of the wave, as it passes from the surface of the plasma to the reflecting layer and back,
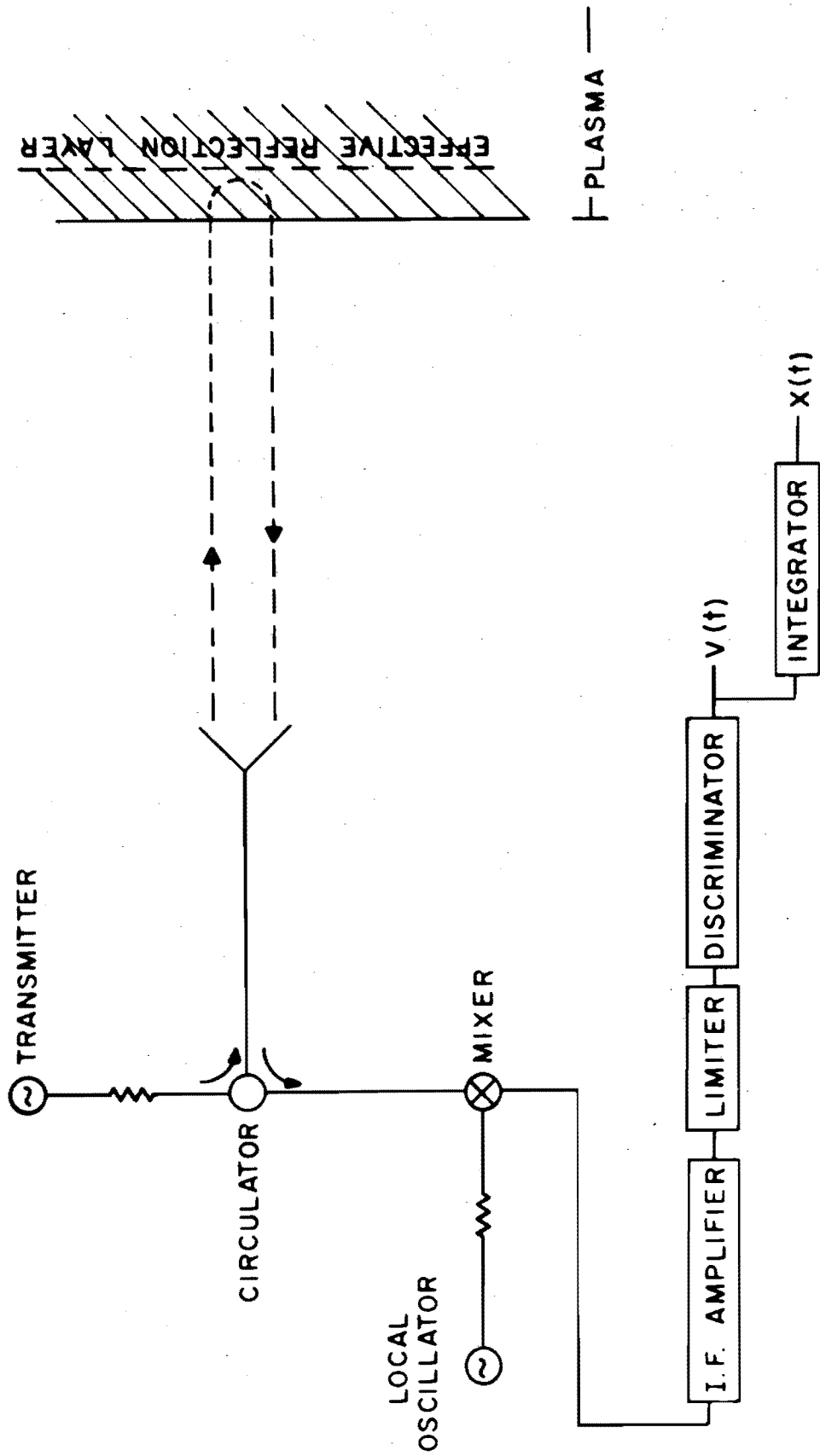
FIG. 12   "DOPPLER RADAR" CIRCUIT FOR MEASURING VELOCITY AND POSITION OF MOVING MIRROR.

is small or at least constant in time.

It is apparent that the measurement of a Doppler-shifted frequency from a moving mirror is closely related to the measurement of the phase-modulation of a signal transmitted through a time-varying plasma, the central problem of electron density measurements. Therefore a circuit analogous to that of Fig. 10, but arranged for transmission instead of reflection and at a higher frequency $\omega > (\omega_p)_{max}$, yields a signal at the integrator output which is proportional to the total phaseshift of the transmitted wave.[48] This class of phase-measuring circuits was mentioned in the section on display circuitry. Conversely, bridge circuits, basic to the measurement of phase, can readily be adapted to measure Doppler shift from a moving mirror.

IV. RADIATION GENERATED BY THE PLASMA

One can generally distinguish between incoherent and coherent radiation from a plasma. The former arises from uncorrelated radiation processes of single particles, and can be interpreted statistically in terms of a "radiation temperature." The latter arises from collective motions of a large number of individual particles and in general has little or no connection with such statistical concepts as temperature. The principal example of coherent processes is the group of disturbances known as plasma oscillations.[10, 71] The interest in thermal radiation at microwave frequencies as a measure of electron temperature arises because of the availability of microwave superhet receivers which are sensitive, have a well-defined bandwidth $d\nu = d\omega/2\pi$ and can easily be built to have fast transient response for use with pulsed discharges. Furthermore, a plasma most closely approximates a blackbody at low frequencies and especially near the plasma and cyclotron frequencies.

A. Models of Thermal Noise

Thermal noise can be studied from several points of view. In the opaque limit, i.e., the sample large compared to a radiation length, the radiation can be evaluated on thermodynamic grounds. The energy density of blackbody radiation is

$$U d\nu \; [\text{joule/m}^3] = 8\pi \frac{h\nu^3}{c^3} \frac{1}{e^{h\nu/kT} - 1} d\nu, \qquad (103)$$

which becomes in the Rayleigh-Jeans limit ($h\nu < < kT$)

$$U d\nu = \frac{8\pi\nu^2 kT}{c^3} \, d\nu = \frac{8\pi kT}{c\lambda^2} \, d\nu \qquad (104)$$

This energy density represents an isotropic flux of electromagnetic energy flowing at velocity c. Thus the radiation intensity into the solid angle d Ω is

$$d^2 I \, [\, \text{watt} /m^2] = c \, U \, \frac{d\Omega}{4\pi} \, . \, d\nu. \qquad (105)$$

Meanwhile the directive properties of a transmitting antenna are specified in terms of a gain function

$$G(\theta, \phi) = \frac{d\psi / d\Omega}{\psi / 4\pi} \qquad (106)$$

where d ψ is the power radiated into the solid angle dΩ in the direction (θ, ϕ) from the antenna and ψ is the total power radiated. The angles θ and ϕ are those of a conventional spherical coordinate system with origin at some convenient point within the antenna, and as usual

$$d\Omega = \sin \theta \, d\theta \, d\phi.$$

Clearly,

$$\frac{1}{4\pi} \oint G(\theta,\phi) \, d\Omega = \oint \frac{d\psi}{\psi} = 1.$$

By reciprocity the angular response of a receiving antenna can be specified in terms of the same gain function. The effective area of a receiving antenna is given by [72]

$$S(\theta,\phi) = G(\theta,\phi) \frac{\lambda^2}{4\pi} . \qquad (107)$$

Since the antenna is sensitive to only one polarization, the total received blackbody power is

$$dP = \frac{1}{2} \cdot \oint_{\Omega} S \, d^2I = \frac{c\lambda^2}{2(4\pi)^2} \, U d\nu \oint G \, d\Omega = \frac{c\lambda^2}{8\pi} \, U \, d\nu = kT \, d\nu .$$

$$(108)$$

For an antenna to deliver to a detector the available noise power $kT \, d\nu$ from a blackbody of finite extent, two conditions must be met:

(a)   the blackbody must be in the far (fraunhofer) field of the antenna

$$R \gtrsim \frac{A^2}{\lambda}$$

(b)   the antenna must "see" only the blackbody

$$2 \frac{\lambda}{A} R \lesssim D_{bb} ,$$

where $2\lambda/A$ is a measure of the angular width of the antenna pattern, and D_{bb} is the dimension of the blackbody. Thus, there is a bound on R

$$A \lesssim \frac{R\lambda}{A} \lesssim \frac{D_{bb}}{2}$$

which may be difficult to meet in practice. One must suitably calibrate the reduction in noise power received if either of the conditions is violated[73].

A second model of plasma noise considers explicitly the fluctuations of the d. c. current in a glow discharge due to the statistics of the individual electron motions between collisions [74]. When such a discharge plasma is matched to a microwave receiver, the available noise power is $kT \, d\nu$ plus a small frequency-dependent term involving the geometry and the d. c. power dissipated in the discharge.

A third model of plasma radiation applies in the transparent limit, when the thickness of the plasma is very small compared to the absorption length. This is bremsstrahlung, i. e., free-free transitions of electrons in the field of the positive ions [24]. The spontaneous emission rate obtained from the Kramers absorption coefficient corrected by the averaged Gaunt factor $\bar{g}(\nu, T)$ is [23, 75].

$$I d\nu \left[\frac{watt}{m^3 - sterad} \right] = \frac{8 \sqrt{2\pi}}{3 \sqrt{3}} \frac{e^6}{(4\pi\epsilon_o)^3 m^{3/2} c^3} \frac{Zn^2}{(kT)^{1/2}} \bar{g}$$

$$\cdot \exp(-h\nu/kT) \, d\nu \qquad\qquad (109)$$

The transition between the transparent and opaque limits for bremsstrahlung radiation from a slab has been treated by Allen and Hindmarsh.[76] They, however, neglect the effects of plasma resonance on radiation near the plasma frequency. Calculations of this sort presuppose Kirchhoff's Law of the equality of emissivity and absorptivity.

We note that the absorption coefficient κ (not corrected for induced emission) and the spontaneous emission intensity I are related by means of Einstein's radiation coefficients,

$$
\left.
\begin{aligned}
\frac{A}{B} &= \frac{2h\nu^3}{c^2} \\[2em]
I_b = \frac{c}{4\pi} \ U &= \frac{2h\nu^3}{c^2} \ \frac{1}{e^{h\nu/kT}-1} \ ,
\end{aligned}
\right\} \qquad (110)
$$

by the relation

$$
\frac{I}{\kappa} = \frac{I_b}{1 + \frac{B}{A} I_b} = \frac{2h\nu^3}{c^2} \ e^{-h\nu/kT} , \qquad (111)
$$

and that the observable absorption coefficient, corrected for induced emmission, is

$$
-\alpha = \kappa - I \frac{B}{A} = \kappa \ (1 - e^{-h\nu/kT}) \ . \qquad (112)
$$

The Kramers formula (with Gaunt factor) being

$$\kappa \ [\ cm^{-1}] \ = \ \frac{4\sqrt{2\pi}}{3\sqrt{3}} \ \frac{e^6}{(4\pi\epsilon_o)^3 m^{3/2} c \ h} \ \frac{Zn^2}{\nu^3 (kT)^{\frac{1}{2}}} \ \overline{g} \ ,$$

(113)

we have for $h\nu << kT$

$$-\alpha[\ cm^{-1}] = \frac{4\sqrt{2\pi}}{3\sqrt{3}} \ \frac{e^6}{(4\pi\epsilon_o)^3 m^{3/2} c} \ \frac{Zn^2}{\nu^2 (kT)^{3/2}} \ \overline{g} \ ,$$

(114)

which is identical with Eq. (18).

A slab is thick enough to approximate a blackbody when

$$-\alpha D \gtrsim 1$$

which requires a low frequency

$$\nu^2 \lesssim \frac{4\sqrt{2\pi}}{3\sqrt{3}} \ \frac{e^6}{(4\pi\epsilon_o)^3 m^{3/2} c} \ \frac{Zn^2 D}{(kT)^{3/2}} \ \overline{g} \ .$$

But to avoid plasma resonance (reactive reflection rather than resistive dissipation),

$$\nu^2 \gtrsim \left(\frac{\omega_p}{2\pi}\right)^2 = \frac{ne^2}{4\pi^2\epsilon_o m} .$$

These two conditions can be met only if

$$\frac{ZnD}{(kT)^{3/2}} \bar{g} \gtrsim \frac{3\sqrt{3}}{4\pi\sqrt{2\pi}} \frac{(4\pi\epsilon_o)^2 m^{\frac{1}{2}}c}{e^4} = 5.68 \ 10^{15} \text{cm}^{-2}\text{ev}^{-3/2} ,$$

(115)

which condition is usually not met in controlled fusion work.

B. Other "Thermal" Radiation Processes

When a hot plasma is located in a magnetic field, the gyration of the electrons gives rise to synchrotron radiation (relativistic cyclotron radiation). [77] Under some conditions this "magnetic bremsstrahlung," which is peaked at harmonics of the cyclotron frequency, can be the dominant radiation process. [78]

Since a plasma in a magnetic field exhibits an index of refraction for certain directions of propagation which is very large, it is possible for fast electrons (at the high-energy end of the thermal distribution) with long mean-free-paths to generate Cerenkov radiation. [28,79] In general it will be peaked near the cyclotron and plasma frequencies. The relation between Cerenkov radiation and ordinary bremsstrahlung has been discussed by Lawson. [80] Cerenkov radiation can also be expected in the presence of a directed stream

of fast, non-thermal electrons, such as arise from the runaway effect.[81]

C. Temperature Measurement from Thermal Noise

Gas discharges have been used for some time as standard noise sources for the microwave region.[82] . We therefore seek means of measuring the electron kinetic temperature of a plasma by means of its thermal radiation.[43, 73, 83] The essential requirements for the application of blackbody concepts are:

1. The radiation must be in equilibrium with the medium; i.e., the

   dimensions of the medium must be large with respect to the radiation

   length (skin depth) for the frequency band in question;

2. The radiation must be able to escape from the medium and dissipate

   itself in the detector.

These conditions are implicit in the absorptivity or emissivity coefficient of Kirchhoff's Law in radiation theory; in electrical engineers' terminology, they are equivalent to saying that the plasma must be matched to the detector. The gas discharges used as microwave noise sources are operated under con-ditions of feeble ionization ($\sim 10^{-6}$) at a moderately high gas pressure (1 - 10 mm Hg). Under these conditions collisions (principally electron-molecule) play a much more dominant role than in the low pressure plasmas we have been considering, and the dissipative absorption is much greater. It is thus possible, using conventional waveguide matching techniques, to match the discharge impedance to the waveguide. One then has, in the Rayleigh-Jeans approximation; an available noise power generated in the waveguide

$$P = kT \ \Delta\nu,$$

where $\Delta\nu$ is the bandwidth of the detector. To demonstrate the applicability of this analysis one performs the following operational test, based on Kirchhoff's Law. Replacing the detector by a signal generator of the appropriate frequency (strictly speaking, frequency band), one must show that the energy produced by the generator is dissipated resistively in the discharge plasma, with neither transmission (condition 1) nor reflection (condition 2').

For typical high-temperature, low-pressure discharges, at lower densities ($n < n_c$) condition (1) is violated, whereas at higher densities ($n > n_c$) condition (2) is violated. The plasma approximates a gray or silver body, respectively. The familiar approach in dealing with gray bodies is to place the object inside an enclosure with perfectly reflecting walls, i.e., a hohlraum, or in microwave terminology a resonant cavity capable of supporting many modes at the frequencies of interest. The radiation is then trapped and forced to come into thermal equilibrium with the plasma. A small sample of the contained radiation is coupled out to an external detector.

We have then the following possibilities in the typical case of a high-temperature, low-pressure plasma:

1. Use a hohlraum approach. For instance, surround a microwave antenna with plasma above critical density and introduce matching devices (discontinuities) in the transmission line between antenna and detector so that the operational test outlined above is satisfied.

2. Arrange to measure the opacity and absorptivity of the plasma directly, thereby calibrating it as a gray body. In the case of a

plasma below critical density, one can apply the theoretical bremsstrahlung flux due to spontaneous emission only as a limiting case for thin samples, if necessary considering also the roles of self-absorption and reemission in the intermediate gray body case.[76] For nearly transparent samples, the energy flux obtained in this way is of course considerably less than that which would be obtained from a blackbody, and therefore the minimum temperature observable with a given apparatus would be correspondingly greater. For thin samples, this effective emissivity factor is[76]

$$\epsilon = -2\alpha D = \frac{2 D}{\delta} << 1. \tag{116}$$

In the case of a plasma above critical density, it is possible that a situation akin to the anamalous skin effect might occur.[84] When the mean free path of electrons in the plasma is greater than the skin depth, the absorptivity of the surface at high frequencies is greater than that inferred from the skin depth alone. However, in the case of a strong magnetostatic field, where the gyroradius would replace the mean free path, this condition might be harder to meet.

The enhanced dissipation to be expected near cyclotron resonance suggests that the plasma emissivity may be high near the cyclotron frequency and the resonance at

$$\omega_{bp} = \sqrt{\omega_b^2 + \omega_p^2}.$$

More precisely, at ω_b and ω_{bp} the index of refraction becomes high, the wavelength short, and an impinging wave is appreciably absorbed before it is reflected by the reactive discontinuity.[43] On the other hand, at the cutoff frequencies

$$\omega_p \quad \text{and} \quad \sqrt{\left(\frac{\omega_b}{2}\right) + \omega_p{}^2} \pm \frac{\omega_b}{2}$$

where the index of refraction goes to zero, the wave largely is reflected before being absorbed unless the density gradient is very low. Indeed the absorption is best when the wave approaches a resonant region ($\mu \rightarrow \infty$) from the high-field side. This consideration means that radiation emerging from a plasma at right-angles to the magnetic field (as usually observed in stellarator geometry) is characterized by a rather low emissivity. However radiation emerging from a plasma into the mirror range of a mirror machine more closely approaches blackbody (for similar conditions of particle densities, density gradients, and temperature). The anisotropic nature of a magnetoplasma raises a number of subtleties, having to due with the validity of Kirchhoff's Law and strong sensitivity to the electron velocity distribution.[85]

D. Non-Thermal Noise

As has been mentioned, plasma oscillations and similar collective processes in plasmas, such as might be associated with instability of plasma confinement, can set up strong internal r.f. electric fields, and in the

presence of a magnetic field or density gradients can radiate energy,[12, 86]

Such coherent noise can be expected to be many orders of magnitude greater

than thermal noise. Certainly high-level microwave noise has been observed

from stellarators.[87] This noise occurs in microsecond bursts, over a wide

spectral range, and is thought to be generated by some process driven by

runaway electron streams.[81] A somewhat similar phenomenon has been

observed from the aurora.[88]

Non-thermal radiation is clearly a useful symptom of whatever

process generates the radiation. However, since at the present time the

physical nature of these processes is not well understood, the observation

of this radiation has not contributed much information on known parameters

of the plasma. It should be noted that non-thermal noise can be expected,

in general, under the more favorable conditions ($\omega \sim \omega_p$ or ω_b) for

observation of thermal noise.

E. Practical Noise Receivers

Microwave receivers can be divided into two classes, video and

superhet.[89] A video receiver is a waveguide-mounted crystal diode de-

tector, which simply rectifies the microwave currents excited in an antenna,

producing a d.c. output voltage when unmodulated microwave power is

incident. At low (microwatt) signal levels the crystal response is app-

roximately "square-law", meaning that the output voltage is proportional

to the square of the microwave amplitude. Thus the detected amplitude is

proportional to r.f. power. The sensitivity varies widely from crystal to

crystal, and with minute changes in the crystal mount. (e.g., removing and reinserting the crystal). At high (milliwatt) signal levels the response approaches linear. The effective internal impedance of a low-level crystal detector is of the order of 10,000 ohms, so that the shunt capacitance of the lead between detector and amplifier input must be limited if high (megacycle) modulation frequencies are to be observed. The microwave frequency response of a video detector is determined by the frequency characteristics of the coupling between waveguide and crystal circuit. Unless special design precuations are taken, the effective sensitivity as a function of frequency is normally a very ragged curve. Thus it is difficult to calibrate (or even define) the effective bandwidth of a waveguide video receiver when used to observe wideband radiation. Video detectors are thus simple, low sensitivity, broadband receivers. Note that bolometers or thermistors may be substituted for crystals, but have limited transient response. Video detectors for short wavelengths (3mm), for which commercial detectors are not yet available, have been discussed by Richardson and Riley.[90]

Superhet receivers employ a local oscillator, mixer, and i.f. amp-lifier, followed by a diode detector at the i.f. frequency. They are char-acterized by high-sensitivity, a well-defined (narrow) bandwidth, and a wide dynamic range of linear response. Normally it is not necessary to reject the image frequency, so that the r.f. (microwave) bandwidth is twice the band-width of the i.f. amplifier, while the transient response is one-half the i.f. bandwidth. Since the i.f. frequency is usually very small compared to the

local oscillator frequency, the local oscillator must be very stable (perhaps automatic-frequency-controlled by a feedback network) to keep a discrete input frequency within the received bandwidth. Normally in noise measurements the bandwidth of the noise is wide enough that frequency stability is no problem. To reduce spurious noise entering on the local oscillator signal, a balanced mixer is often used.[91] Noise figures in millimeter superhet receivers vary between 10 and 25 db, depending on the frequency. Harmonic local oscillators can be used for the higher frequencies, for which fundamental oscillators are not available.[92] Receivers can be calibrated by means of commercial gas-discharge noise sources.

Because controlled fusion work normally deals with one-shot pulsed plasmas, the Dicke radiometer type of receiver, which uses synchronous detection and a long integrating time to observe very low-level thermal noise, is usually not of interest.[93].

Appendix

NOTION OF COMPLEX CONDUCTIVITY

We here recapitulate the well-known arguments leading to the concepts

of complex dielectric constant and conductivity.

Amperes Law

$$\nabla \times H = J + D \qquad \text{(mks units)}$$

becomes for simple harmonic fields varying as

$$\exp (-i\omega t + \gamma x),$$

$$\nabla \times H = \sigma E - i\omega (\epsilon_o E + P)$$

$$= \sigma E - i\omega K \epsilon_o E$$

where σ is the conductivity and K the dielectric constant. The properties

of the medium, σ and K, are taken to be functions of frequency. Frequently

it is helpful to incorporate one of these constants in the other by means of

complex notation, which is readily done since they represent respectively

resistive and reactive processes.

In the case of dielectrics, it is customary to put

$$(\sigma - i\omega K \epsilon_o) E = - i\omega K * \epsilon_o E$$

or

$$K* \doteq K + i \frac{\sigma}{\omega \epsilon_o} = K' + i K''. \qquad (A-1)$$

The "loss tangent" for a dielectric material is defined as

$$\tan \delta \equiv \frac{\kappa''}{\kappa'}.$$ (A-2)

Note that the a.c. κ'' may include hidden dissipative currents (such as dielectric hysteresis loss) in addition to currents resulting from d.c. conductivity.

The (complex) propagation constant is

$$\gamma \equiv \alpha + i\beta = i\sqrt{\kappa^* \epsilon_o \mu_o} \ \omega = i\sqrt{\kappa^*} \ \frac{\omega}{c}$$ (A-3)

Thus for $\kappa' \gg \kappa''$ (low-loss dielectric)

$$\frac{\gamma c}{\omega} \to i\sqrt{\kappa'},$$ (A-4)

and for $\kappa' \ll \kappa''$ (metallic conductor)

$$\frac{\gamma c}{\omega} \quad i\sqrt{i\kappa''} = -\sqrt{\frac{\kappa''}{2}} + i\sqrt{\frac{\kappa''}{2}},$$ (A-5)

since

$$\sqrt{i} = \frac{1 + i}{\sqrt{2}} \qquad .$$

since $(-\alpha)$ is the reciprocal of the skin depth or radiation length δ, for this latter case

$$\delta = \frac{c}{\omega} \sqrt{\frac{2}{\kappa''}} = \frac{c}{\omega} \sqrt{2\left(\frac{\omega \epsilon_o}{\sigma}\right)} = \sqrt{\frac{2}{\mu_o \omega \sigma}} , \qquad (A-6)$$

the usual formula for conductors.

In the case of ionized gases, it is customary to employ a complex conductivity

$$(\sigma - i\omega\kappa\epsilon_o) E \equiv (\sigma^* - i\omega\epsilon_o) E$$

or

$$\sigma^* \equiv \sigma - i\omega a \equiv \sigma_r - i\sigma_i , \qquad (A-7)$$

where a is the electric susceptibility from

$$P = aE .$$

For this notation we have

$$\kappa^* = 1 + \frac{\sigma_i}{\omega\epsilon_o} + i \frac{\sigma_r}{\omega\epsilon_o} . \qquad (A-8)$$

The propagation constant for the special case

$$\kappa' = 1 + \frac{\sigma_i}{\omega \epsilon_o} < 0 ; \quad \kappa'' = \frac{\sigma_r}{\omega \epsilon_o} \approx 0$$

is

$$\frac{\gamma c}{\omega} = i\sqrt{\kappa*} = -\sqrt{|\kappa'|} \tag{A-9}$$

That is, the medium attenuates without phase shift, corresponding more closely to a waveguide beyond cut-off than to a metallic conductor.

REFERENCES

1. L. Tonks and I. Langmuir, "Oscillations in Ionized Gases," Phys. Rev. 33, 195, 990 (1929).

2. J. A. Stratton, Electromagnetic Theory (McGraw-Hill, 1941), pp. 327-30.

3. H. R. Mimno, "The Physics of the Ionosphere," Rev. Mod. Phys. 9, 1 (1937).

4. S. K. Mitra, The Upper Atmosphere (The Asiatic Society, Calcutta, 1952), second edition; J. A. Ratcliffe, The Magneto-Ionic Theory and Its Applications to the Ionosphere (Cambridge, 1959).

5. J. L. Pawsey and R. N. Bracewell, Radio Astronomy (Oxford, 1955).

6. L. Goldstein, "Electrical Discharge in Gases and Modern Electronics," advances in Electronics and Electron Physics 7, 399 (1955).

7. T. G. Cowling, Magnetohydrodynamics (Interscience, 1957).

8. Bohm, Burhop, and Massey, "The Use of Probes for Plasma Exploration in Strong Magnetic Fields," Chap. 2 of Guthrie and Wakerling, Characteristics of Electrical Discharges in Magnetic Fields, (McGraw-Hill, 1949).

9. J. M. Dawson, "Nonlinear Electron Oscillations in a Cold Plasma," Phys. Rev. 113, 383 (1959); Section V.

10. L. Spitzer, Physics of Fully Ionized Gases (Interscience, 1956), Section 4.3.

11. R. W. Gould and A. W. Trivelpiece, "A New Mode of Wave Propagation on Electron Beams," Proc. of Symposium on Electronic Waveguides (Polytechnic Institute of Brooklyn, 1958), p. 215; L. D. Smullin and P. Chorney, "Propagation in Ion Loaded Waveguides," Ibid., p. 229.

12. J. Dawson and C. Oberman, "Oscillations of a Finite Cold Plasma in a Strong Magnetic Field," Phys. Fluids 2, 103 (1959).

13. G. M. Branch and T. G. Mihran, "Plasma Frequency Reduction Factors in Electron Beams," Trans. IRE PGED 2, No. 2, 3 (1955).

14. S. J. Buchsbaum and S. C. Brown, "Microwave Measurements of High Electron Densities," Phys. Rev. 106, 196 (1957).

15. H. Margenau, "Conductivity of Plasmas to Microwaves," Phys. Rev. 109, 6 (1958).

16. E. A. Desloge, S. W. Matthysse, and H. Margenau, "Conductivity of Plasmas to Microwaves," Phys. Rev. 112, 1437 (1959).

17. J. M. Anderson and L. Goldstein, "Interaction of Electromagnetic Waves of Radio-Frequency in Isothermal Plasmas: Collision Cross Section of Helium Atoms and Ions for Electrons," Phys. Rev. 100, 1037 (1955).

18. V. Ginsburg, "On the Absorption of Radio Waves and the Number of Collisions in the Ionosphere," J. Phys. (USSR) 8, 253 (1944); P. Molmud, "Langevin Equation and the AC Conductivity of Non-Maxwellian Plasmas," Phys. Rev. 114, 29 (1959).

19. H. Margenau, "Conduction and Dispersion of Ionized Gases at High Frequencies," Phys. Rev. 69, 508 (1946); P. H. Fang, "Conductivity of Plasmas to Microwaves," Phys. Rev. 113, 13 (1959).

20. Reference 10, Chap. 5.

21. R. C. Hwa, "Effects of Electron-Electron Interactions on Cyclotron Resonances in Gaseous Plasmas," Phys. Rev. 110, 307 (1958).

22. H. De Witt, "The Free-Free Absorption Coefficient in Ionized Gases," USAEC Rept. UCRL-5377 (October 1958).

23. J. A. Gaunt, "Continuous Absorption," Phil. Trans. Roy. Soc. Lon. A229, 163 (1930); Section 6.4.

24. J. Greene, "Bremsstrahlung from a Maxwellian Gas," USAEC Rept. NYO-7905 (November 1958).

25. W. P. Allis, "Motions of Ions and Electrons," Handbuch der Physik (Springer, 1956), Vol. 21, p. 383; reprinted as MIT Research Laboratory of Electronics Tech. Rept. 299 (June 1956); C. H. M. Turner, "Birefringence in Crystals and in the Ionosphere," Can. J. Phys. 32, 16 (1954).

26. L. Goldstein, "Nonreciprocal Electromagnetic Wave Propagation in Ionized Gaseons Media," Trans. IRE PGMTT 6 19 (1958).

27. L. Mower, "Propagation of Plane Waves in an Electrically Anisotropic Medium," Sylvania Microwave Physics Laboratory Report MPL-1 (November 1956).

28. J. V. Jelley, Cerenkov Radiation (Pergamon, 1958).

29. P. Rosen, "Electromagnetic Waves in an Ionized Gas," Phys. Rev. 103, 390 (1956).

30. J. E. Drummond, "Basic Microwave Properties of Hot Magnetoplasmas," Phys. Rev. 110, 293 (1958); J. E. Drummond, "Microwave Propagation in Hot Magnetoplasmas," Phys. Rev. 112, 1460 (1958).

31. M. E. Gertsenshtein, "Dielectric Permeability of Plasma Located in a Stationary Magnetic Field," Zh. eksper. teor. Fiz. 27, 180 (1954); T. Pradhan, "Plasma Oscillations in a Steady Magnetic Field: Circularly Polarized Electromagnetic Modes," Phys. Rev. 107, 1222 (1957).

32. I. B. Bernstein, "Waves in a Plasma in a Magnetic Field," Phys. Rev. 109, 10 (1958).

33. C. G. Darwin, "The Refractive Index of an Ionized Medium," Proc. Roy. Soc. A146, 17 (1934).

34. E. Astrom, "On Waves in an Ionized Gas," Arkiv Fysik 2, 443 (1950); Auer, Hurwitz, and Miller, "Collective Oscillations of a Cold Plasma," Phys. Fluids 1, 501 (1958); Hall, Gardner, and Fundingsland, "Analysis of the Interaction of Electromagnetic Radiation with a Plasma in a Magnetic Field," USAEC Report UCRL-4744 (September 1956).

35. Reference 10, Section 3.1(d).

36. E. Astrom, "Waves in a Hot Ionized Gas in a Magnetic Field," in Electromagnetic Phenomena in Cosmical Physics, B. Lehnert, Ed. (Cambridge, 1958), p. 81.

37. A. A. Van Trier, "Guided Electromagnetic Waves in Anisotropic Media," Appl. Sci. Res. B3, 305 (1953); H. Suhl and L. R. Walker, "Topics in Guided Propagation through Gyromagnetic Media," Bell Syst. Tech. J. 33, 579, 939, 1133 (1954); P. S. Epstein, "Theory of Wave Propagation in a Gyromagnetic Medium," Rev. Mod. Phys. 28, 3 (1956); B. Agdur, "Notes on the Propagation of Guided Microwaves through an Electron Gas in the Presence of a Static Magnetic Field," Proc. of Symposium on Electronic Waveguides (Polytechnic Inst. of Brooklyn, 1958), p. 177. Note that treatments of gyromagnetic problems (e.g., ferrites) are applicable to the gyroelectric plasma case because of the symmetry of Maxwell's equations.

38. S. C. Brown, "The Interaction of Microwaves with Gas-Discharge Plasmas," Trans. IRE PGMTT 7, 69 (1959).

39. M. A. Biondi, "Measurement of the Electron Density in Ionized Gases by Microwave Techniques," Rev. Sci. Inst. 22, 500 (1951); S. C. Brown, D. J. Rose, and L. Gould, "Methods of Measuring the Properties of Ionized Gases at High Frequencies," J. Appl. Phys. 23, 711, 719, 1028 (1952); 24, 1053 (1953); H. J. Oskam, "Microwave Investigation of Disintegrating Gaseous Discharge Plasmas," Thesis, Univ. of Utrecht (November 1957).

40. J. C. Slater, "Microwave Electronics," Rev. Mod. Phys. 18, 441 (1946).

41. K. B. Persson, "Limitations of the Microwave Cavity Method of Measuring Electron Densities in a Plasma," Phys. Rev. 106, 191 (1957).

42. M. A. Heald, "The Use of TE_{0M1} Cavities for Density Measurements in Stellarators," Project Matterhorn Tech. Memo. 80 (July 1959).

43. C. B. Wharton, "Microwave Diagnostics for Controlled Fusion Research," USAEC Report UCRL-4836 (Rev.) (September 1957).

44. R. F. Whitmer, "Microwave Studies of the Electron Loss Processes in Gaseous Discharges," Phys. Rev. 104, 572 (1956); W. W. Balwanz, "Studies of Combustion Zone Ionization Utilizing Focused Electromagnetic Beams," Bull. Amer. Phys. Soc. 2, 84 (1957).

45. Reference 2, pp. 511-16.

46. C. B. Wharton and D. M. Slager, "Microwave Interferometer Measurements for the Determination of Average Electron Density and of Density Profiles in Plasmas," USAEC Reports UCRL--5244 (June 1958) and UCRL-5400 (November 1958); R. Motley and M. A. Heald, "Use of Multiple Polarizations for Electron Density Profile Measurements in High-Temperature Plasmas," Proc. of Symposium on Millimeter Waves (Polytechnic Inst. of Brooklyn, 1959), in press.

47. M. A. Heald, "Engineering Design of Microwave Electron Density Measuring Systems," Project Matterhorn Tech. Memo 78 (July 1959).

48. Project Matterhorn Quarterly Report PM-Q-2, USAEC Report NYO-2193 (March 1958), pp. 12-13.

49. E. J. Faust, "An Automatic Microwave Phase-Measuring Circuit with Linear Voltage Output," M. S. thesis, University of Pennsylvania (June 1959); M. J. Kofoid, "Automatic Measurement of Phase Retardation for Radome Analysis," Rev. Sci. Instr. 27, 450 (1956).

50. M. A. Heald, "Proposal for a New Type of Phase-Measuring System having an output voltage proportional to Phaseshift," Project Matterhorn Microwave Memo No. 4 (July 1959).

51. See for instance Polytechnic Research and Development Co. Catalog E-8 (1959); p. I-16.

52. C. L. Andrews, "Diffraction Pattern of a Circular Aperture at Short Distances," Phys. Rev. 71, 777 (1947).

53. G. Bekefi, "Studies in Microwave Optics," E. E. R. L. Tech. Rept. No. 38, McGill University (March 1957).

54. C. G. Montgomery (Ed.), Technique of Microwave Measurements, MIT Radiation Laboratory Series, Vol. 11 (McGraw-Hill, 1947); Chapter 15.

55. R. B. Barrar and Wilcox, "On the Fresnel Approximation," Trans. IRE PGAP 6, 43 (1958).

56. M. H. Brown, "Fresnel Region Properties of Millimeter Antennas," First Tri-Service Millimeter Wave Symposium, Ft. Monmouth (September 1957).

57. W. Culshaw, "Diffraction Corrections in Microwave Optics," NBS Report 5578 (July 1958).

58. C. Froese and J. R. Wait, "Calculated Diffraction Patterns of Dielectric Rods at Centimetric Wavelengths," Can. J. Phys. 32, 775 (1954); H. Wilhelmsson, "On the Reflection of Electromagnetic Waves from a Dielectric Cylinder," Trans. Chalmers Univ. of Tech., Gothenburg, Sweden, No. 168 (1955).

59. K. M. Siegel, "Far Field Scattering from Bodies of Revolution," Appl. Sci. Res. B7, 293 (1959).

60. F. V. Bunkin, "On Radiation in Anisotropic Media," Soviet Physics JETP 5, 277 (1957).

61. R. M. Redheffer, "Microwave Antennas and Dielectric Surfaces," J. Appl. Phys. 20, 397 (1949).

62. B. B. Rosen, "The 'Inverted-Universe' Plasma Analog for Microwaves," Project Matterhorn Tech. Memo 85 (August 1959).

63. H. Iams, "A Method of Simulating Propagation Problems," Proc. I.R.E. 38, 543 (1950).

64. B. B. Rosen, unpublished data.

65. S. A. Schelkunoff and H. T. Friis, <u>Antennas: Theory and Practice</u> (Wiley, 1952); Chap. 16, especially pp. 528-9 and 601.

66. F. E. Boyd, "Converging Lens Dielectric Antennas," NRL Report 3780 (December 1950).

67. M. D. Fiske, "Resonant Windows for Vacuum Seals in Rectangular Waveguides," Rev. Sci. Instr. <u>17</u>, 478 (1946); G. B. Collins (Ed.), <u>Microwave Magnetrons</u>, MIT Radiation Laboratory Series, Vol. 6 (McGraw-Hill, 1948), pp. 487-8.

68. D. J. Grove, "The Application of Ultra-High Vacuum Techniques to Controlled Thermonuclear Devices," USAEC Report NYO-8750 (October 1958).

69. S. P. Morgan, "General Solution of the Luneberg Lens Problem," J. Appl. Phys. <u>29</u>, 1358 (1958).

70. H. Osterberg, "Propagation of Plane Electromagnetic Waves in Inhomogeneous Media," J. Opt. Soc. Amer. <u>48</u>, 513 (1958).

71. D. Bohm and E. P. Gross, "Theory of Plasma Oscillations," Phys. Rev. <u>75</u>, 1851, 1864 (1949).

72. Reference 65, pp. 43-4 and Chap. 6.

73. Bekefi, Hirshfield and Brown, "Incoherent Microwave Radiation from Plasmas," to be published.

74. P. Parzen and L. Goldstein, "Current Fluctuations in the Direct-Current Gas Discharge Plasma," Phys. Rev. <u>82</u>, 724 (1951).

75. H. A. Kramers, "On the Theory of X-Ray Absorption and of the Continuous X-Ray Spectrum," Phil. Mag. <u>46</u>, 836 (1923); G. Cillie, "The Hydrogen Emission in Gaseous Nebulae," Mon. Not. Roy. Ast. Soc. <u>92</u>, 820 (1932); W. B. Thompson, "Radiation from a Plasma," UK AERE Report T/M-73 (September 1954).

76. J. E. Allen and W. R. Hindmarsh, "The Bremsstrahlung Radiation from Ionized Hydrogen," UK AERE Report GP/R-1761 (September 1955).

77. J. Schwinger, "On the Classical Radiation of Accelerated Electrons," Phys. Rev. <u>75</u>, 1912 (1949).

78. B. A. Trubnikov and V. S. Kudryavtsev, "Plasma Radiation in a Magnetic Field," Proc. Geneva Conf. <u>31</u>, 93 (1958); D. B. Beard, "Cyclotron Radiation from Magnetically Confined Plasmas," Phys. Fluids <u>2</u>, 379 (1959).

79. A. A. Kolomenskie, "Radiation from a Plasma Electron in Uniform Motion in a Magnetic Field," Soviet Physics Doklady <u>1</u>, 133 (1956).

80. J. D. Lawson, "On the Relation Between Cerenkov Radiation and Bremsstrahlung," Phil. Mag. <u>45</u>, 748 (1954).

81. H. Dreicer, "Electron and Ion Run-Away in a Fully Ionized Gas," Phys. Rev. to be published; Bernstein, Chen, Heald, and Kranz, " 'Runaway' Electrons and Cooperative Phenomena in B-1 Stellarator Discharges," Phys. Fluids <u>1</u>, 430 (1958).

82. K. S. Knol, "Determination of the Electron Temperature in Gas Discharges by Noise Measurements," Philips Res. Rept. 6, 288 (1951); H. Johnson and K. R. Deremer, "Gaseous Discharge Super-High-Frequency Noise Sources," Proc. IRE 39, 908 (1951); L. W. Davies and E. Cowcher, "Microwave and Meter Wave Radiation from the Positive Column of a Gas Discharge," Aust. J. Phys. 8, 108 (1955).

83. A. N. Dellis, "The Measurement of Electron Temperatures by Microwave Methods," UK AERE Rept. GP/R-2265 (May 1957).

84. M. A. Biondi, "Optical Absorption of Copper and Silver at 4.2°K," Phys. Rev. 102, 964 (1956).

85. F. V. Bunkin, "Thermal Radiation from an Anisotropic Medium," Soviet Physics JETP 5, 665 (1957).

86. G. B. Field, "Radiation by Plasma Oscillations," Astrophys. J. 124, 555 (1956).

87. M. A. Heald, "Microwave Generation in B-1," Proc. of Conference on Controlled Thermonuclear Reactions, USAEC Report T1D-7520 (September 1956), pp. 202-6.

88. Forsyth, Petrie, and Currie, "On the Origin of Ten-Centimeter Radiation from the Polar Aurora," Can. J. Res. A28, 324 (1950).

89. S. N. VanVoorhis (Ed.), Microwave Receivers, MIT Radiation Laboratory Series, Vol. 23 (McGraw-Hill, 1948).

90. J. M. Richardson and R. B. Riley, "Performance of Three-Millimeter Harmonic Generators and Crystal Detectors," Trans. IRE PGMTT 5, 131 (1957).

91. J. B. Newman and M. Cohn, "Microwave Mixer Performance at High Intermediate Frequencies," Johns Hopkins Univ. Radiation Laboratory Report AF-51 (June 1958).

92. C. M. Johnson, "Superheterodyne Receiver for the 100 to 150-KMC Region," Trans. IRE PGMTT 2, 27 (1954).

93. R. H. Dicke, "The Measurement of Thermal Radiation at Microwave Frequencies," Rev. Sci. Instr. 17, 268 (1946).